DOI: 10.1002/cmdc.201100054

Inhibition of Xanthine Oxidase by Thiosemicarbazones, Hydrazones and Dithiocarbazates Derived from Hydroxy-Substituted Benzaldehydes

Maria Leigh,[a] Daniel J. Raines,[a] Carmen E. Castillo,[a, b] and Anne K. Duhme-Klair*[a]

Nonpurine xanthine oxidoreductase (XOR) inhibitors represent important alternatives to the purine analogue allopurinol, which is still the most widely used drug in the treatment of conditions associated with elevated uric acid levels in the blood. By condensing mono-, di- and trihydroxybenzaldehydes with aromatic thiosemicarbazides, aryl hydrazides and dithiocarbazates, three series of structurally related Schiff bases were synthesised, characterised and tested for XOR inhibitory activity. Hydroxy substitution in the *para*-position of the benzaldehyde component was found to confer high inhibitory activities. Acyl hydrazones were generally less potent than thiocarbonyl-containing Schiff bases. Within the thiosemicarbazone series, chloro and cyano substituents in the *para*-position of the thiosemicarbazide unit increased activities further, up to potencies approximately four-times higher than that of the benchmark allopurinol, as measured under the same assay conditions. In order to illustrate the potential of the Schiff bases to bind directly to the molybdenum centre in the active site of the enzyme, a representative example (H_2L) of each inhibitor series was co-ordinated to a *cis*-dioxomolybdenum(VI) unit, and the resulting complexes, [MoO_2(L)MeOH], were structurally characterised. Subsequent steady-state kinetic investigations, however, indicated mixed-type inhibition, similar to that observed for inhibitors known to bind within the substrate access channel of the enzyme, remote from the Mo centre. Enzyme co-crystallisation studies are thus required to determine the exact binding mode. Finally, the coordination of representative inhibitors to copper(II) gave rise to significantly decreased IC_{50} values, revealing an additive effect that merits further investigation.

Introduction

Xanthine oxidoreductase (XOR) inhibitors are widely used in the control of uric acid blood levels.[1] High uric acid concentrations (hyperuricemia) can lead to the formation of monosodium urate crystals in the joints and surrounding tissues, leading to the inflammation and pain associated with gout. In addition, monosodium urate may accumulate in the kidneys, resulting in the development of nephrolithiasis.[2]

Mammalian XOR exists in two interconvertible forms, xanthine dehydrogenase (XDH; EC 1.17.1.4) and xanthine oxidase (XO; EC 1.17.3.2). Both forms are involved in the catabolism of dietary and endogenous purines by catalysing the hydroxylation of hypoxanthine to xanthine and xanthine to uric acid (Scheme 1).[2b,3] Initially, the XDH form of the enzyme is produced, which uses NAD^+ as a terminal electron acceptor. In tissues, however, XDH can be converted to XO, which uses dioxygen as its final electron acceptor.[2a,4] The latter produces superoxide and hydrogen peroxide, which can be converted to other more damaging reactive oxygen species (ROS), such as hydroxyl radicals or peroxynitrite.[4,5] XO inhibitors may, therefore, find additional applications in the treatment of conditions associated with radical-induced tissue damage and oxidative stress, including ischemia–reperfusion injury, chronic heart failure and vascular disease.[2a]

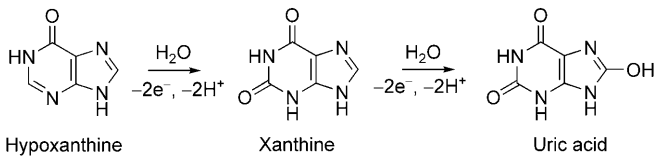

Scheme 1. Formation of uric acid catalysed by xanthine oxidase.[2a]

Although discovered more than 40 years ago, the purine analogue allopurinol is still the most commonly prescribed XOR inhibitor. However, side effects, such as skin rashes, gastrointestinal problems and drowsiness, are not uncommon. Severe hypersensitivity to allopurinol has also been reported, mainly in patients with renal insufficiency.[2a,6] The implication of toxic metabolites of purine analogues in adverse effects prompted the development of alternative structural scaffolds for XOR inhibitors.[7] Several of these nonpurine scaffolds have given rise to derivatives with remarkable in vitro inhibitory activities.[1] Of these, a number of structurally related drug candidates featuring an aromatic nitrile linked in the *meta*-position to a five-membered, unsaturated heterocycle showed hypouricemic ef-

[a] *M. Leigh, D. J. Raines, Dr. C. E. Castillo, Dr. A. K. Duhme-Klair*
Department of Chemistry, University of York
Heslington, York, YO10 5DD (UK)
Fax: (+44) 1904 322516
E-mail: anne.duhme-klair@york.ac.uk

[b] *Dr. C. E. Castillo*
Departamento de Ciencia de los Materiales e Ingeniería Metalúrgica
Y Química Inorgánica, Facultad de Ciencias, Universidad de Cádiz
Polígono Rio San Pedro, 11510 Puerto Real, Cádiz (Spain)

fects in vivo that merited further progression into preclinical or even clinical studies.

Notable compounds within this series of potent nonpurine XO inhibitors include Y-700 (Pyranostat) synthesised by Ishibuchi and co-workers,[8] the particularly potent inhibitor Fyx-

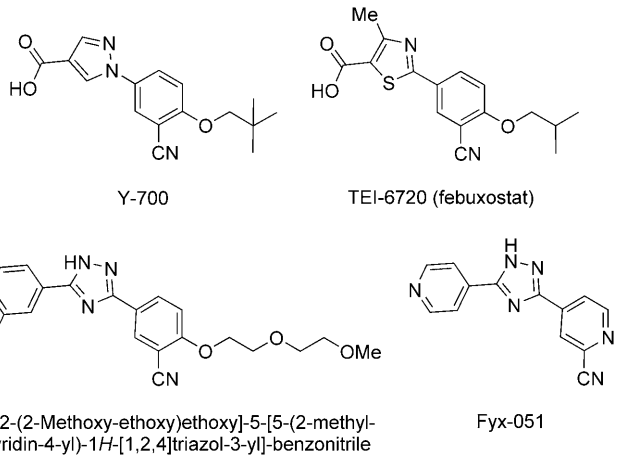

051,[9] which combines a pyridyl-triazole scaffold that resembles the one initially developed by Baldwin et al.[10] with the use of a *meta*-cyanopyridyl fragment similar to the *meta*-cyanophenyl substituent seen in Y-700 and 2-[2-(2-methoxy-ethoxy)-ethoxy]-5-[5-(2-methyl-pyridin-4-yl)-1*H*-[1,2,4]triazol-3-yl]-benzonitrile, a recently reported, related drug candidate with potent in vivo activity but only moderate pharmacokinetic profile.[11] The first and only nonpurine-type inhibitor to obtain market approval in the EU and USA in 2008 and 2009, respectively, is 2-(3-cyano-4-isobutoxyphenyl)-4-methyl-1,3-thiazole-5-carboxylic acid (TEI-6720 or febuxostat, brand names: Adenuric (EU) and Uloric (USA)). Since long-term safety data are not yet available, and adverse effects, including altered liver function, have been reported, use of febuxostat in the UK is recommended in cases where allopurinol is contra-indicated or poorly tolerated.[12]

As reported in previous studies, the presence of hydroxy substituents is linked to potent XO inhibition.[13] Naturally oc-

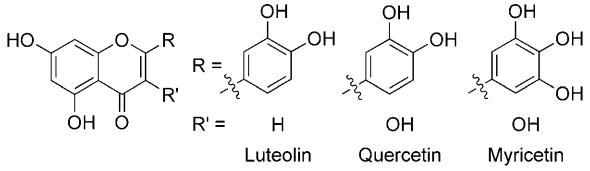

curring phenolic compounds, such as luteolin, quercetin and silibinin, have been shown to inhibit XO effectively, acting as competitive or mixed-type inhibitors.[13c] Comparison of the structurally related flavonoids quercetin, luteolin and myricetin, revealed that the position and the number of hydroxy substituents greatly influences potency, as the inhibitory activity decreased in the order of quercetin > luteolin > myricetin.[14] Extracts derived from plants traditionally used as antigout and antirheumatic therapeutics have shown that the inhibitory activity increases moderately with phenolic content.[15] Reported work using docking studies has led to the hypothesis that the phenolic moiety projects into the solvent channel of the enzyme, potentially stabilising the position of the inhibitor via hydrogen bonding and electrostatic interactions with key amino acid residues such as Arg 880, Glu 1261 and Thr 1010.[13c,16]

We have recently communicated the first account of promising XO inhibitory activity exhibited by selected thiosemicarbazones derived from 2,4,6-trihydroxybenzaldehyde (Scheme 2;

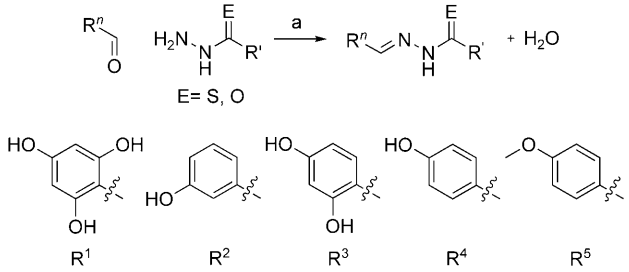

Scheme 2. General synthetic approach to Schiff bases using a variety of substituted benzaldehydes and a selection of NH_2-containing compounds. *Reagents and conditions:* a) EtOH, reflux, 4 h, 40–95%.

R^1, E = S) and aromatic thiosemicarbazides.[17] In this paper, we now report further insights into the underlying structure–activity relationships (SARs) gained by investigating a wider variety of substituents in the *ortho-*, *meta-* and *para*-positions of both aromatic components (R^n and R′) of related thiosemicarbazones, hydrazones and dithiocarbazates.

In particular, in view of the importance of phenols, as highlighted in the literature, the *number* and *position* of hydroxy substituents on the benzaldehyde compounds were investigated (Scheme 2; R^{1-5}). The synthesis, characterisation and inhibitory activity of a number of such compounds are reported herein. The SAR data obtained are compared with those reported for other nonpurine XOR inhibitors that contain aromatic components with similar substitution patterns, including febuxostat, Schiff base metal complexes,[18] chalcone derivatives,[19] and naturally occurring XOR inhibitors, such as flavonoids.[13c]

The NH_2-containing components chosen for this study contained sulfur and NH groups, as well as hydroxy and cyano aromatic substituents. These functionalities are known to contribute to potent XO inhibition through favourable stabilising hydrogen-bond interactions with amino acid residues in the access channel leading to the active site. Sulfur donors in thiosemicarbazones and dithiocarbazates were chosen due to the known thiophilicity of molybdenum and also to allow direct comparison with oxygen-containing Schiff base counterparts (hydrazones).[6,9a,20]

Results and Discussion

Chemistry

The synthesis of the Schiff bases involved refluxing equimolar amounts of the appropriate benzaldehyde with the respective thiosemicarbazide, aryl hydrazide or dithiocarbazate, in ethanol. After 4 h, precipitated products were isolated. If no precipitate was formed, the products were obtained after partial evaporation of the solvent or precipitation with a minimum amount of water. The Schiff bases were washed with ethanol and dried in vacuo. Evidence of successful condensation leading to Schiff base formation was obtained by the appearance of the ^{1}H NMR spectroscopic signature of the new imine bond, characterised by a singlet resonance of the imine proton appearing at 8.05–8.65 ppm. The disappearance of the signature of the aldehyde proton in the ^{1}H NMR spectra of compounds reported herein provided further evidence of Schiff base formation. The imine carbon resonance appeared at 140.80–149.40 ppm in the ^{13}C NMR spectra, and a $\tilde{\nu}$(C=N) band appeared at 1578–1643 cm^{-1} in the Fourier-transform infrared (FTIR) spectra of the compounds. All Schiff bases proved soluble in acetone, methanol, dimethyl sulfoxide (DMSO) and *N,N*-dimethylformamide (DMF).

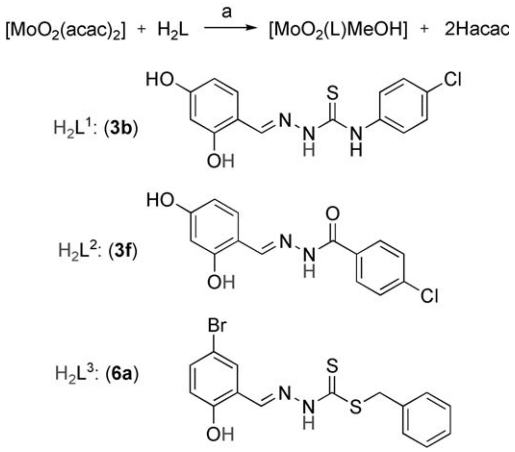

Scheme 3. General synthesis of Mo^{VI} Schiff base complexes from [MoO_2(acac)$_2$]. *Reagents and conditions:* a) MeOH, reflux, 45–89%.

Molybdenum(VI) complexation studies

Molybdenum complexes of Schiff base ligands with ONO and ONS donors have been designed and used as models for studying active sites and reactions of biological importance.[21] In order to probe the potential of direct coordination to a Mo^{VI} centre, a representative compound from each class of Schiff bases, derivatives **3b**, **3f** and **6a**, was reacted with dioxomolybdenum(VI) acetylacetonate ([MoO_2(acac)$_2$]; Scheme 3). The *cis*-MoO_2^{2+} moiety of [MoO_2(acac)$_2$] was chosen to mimic the oxo and thio groups attached to the Mo^{VI} in the active site of the enzyme.[21b,d,22] All Schiff bases readily formed mononuclear Mo^{VI} complexes, [MoO_2(L)MeOH], with the carbonyl/thiocarbonyl heteroatom, imine nitrogen, and phenolate oxygen in the *ortho*-position acting as donor atoms of the tridentate ligands. The potential of direct coordination of inhibitors to the Mo^{VI} active site of XO can lead to longer lasting and more potent inhibition, as seen with allopurinol and Fyx-051.[9a,23]

The molybdenum complexes were characterised by NMR, FTIR, UV/vis spectroscopy and X-ray diffraction. Evidence of complexation was observed through the disappearance of two singlet resonances assigned to NH and OH in the ^{1}H NMR spectra of the ligands as a consequence of coordination to the Mo^{VI} centre. The presence of the coordinated methanol solvent molecule was indicated by the appearance of resonances at 3.17 and 4.10 ppm.[21e,22,24]

Electronic absorption spectra were recorded for all complexes and their free ligands in DMSO (Table 1). The absorption bands at 335–366 nm for H_2L^n are attributed to n→π* intraligand transitions, while bands ≤313 nm arise due to intraligand π→π* transitions.[21d,25] Upon complexation, the n→π* bands experienced a shift to a shorter wavelength (326–340 nm), as the two intraligand bands merged. The appearance of a new LMCT band from the ligand O, N or S donors to the molybdenum centre in [MoO_2(L^n)MeOH] at approximately 430 nm, confirmed coordination to the Mo^{VI} centre.[24b,26]

Additionally, FTIR spectroscopic data (Table 2) confirmed coordination, with $\tilde{\nu}$(C=N) shifting to a lower wavenumber as compared to the free ligand, indicating redistribution of electron density. A shift was also observed for the phenolic $\tilde{\nu}$(C–O), indicating participation of the phenolate donor in

Table 1. ^{1}H NMR and UV/vis spectroscopic data of selected Schiff base ligands and their Mo^{VI} complexes.

Compd	^{1}H NMR: δ [ppm]		UV/vis: λ_{max} [nm], ε [mol^{-1} L cm^{-1}]		
H_2L^1	8.36	(*CH*N)	293, 14482	308, 15190	350, 30722
	9.82, 9.87, 9.96, 11.66	(*OH*/N*H*)			
[MoO_2(L^1)MeOH]	8.66	(*CH*N)	340, 25460	428, 5580	
	9.63, 10.44	(*OH*/N*H*)			
	3.17, 4.10	(*CH*$_3$*OH*)			
H_2L^2	8.48	(*CH*N)	292, 11052	304, 14980	335, 28702
	9.99, 11.39, 11.97	(*OH*/N*H*)			
[MoO_2(L^2)MeOH]	8.78	(*CH*N)	326, 23590	421, 7957	
	10.64	(*OH*/N*H*)			
	3.15, 4.09	(*CH*$_3$*OH*)			
H_2L^3	8.43	(*CH*N)	313, 11205	366, 21654	
	10.53, 11.28	(*OH*/N*H*)			
[MoO_2(L^3)MeOH]	9.01	(*CH*N)	329, 16656	438, 1033	
	–	(*OH*/N*H*)			
	3.17, 4.11	(*CH*$_3$*OH*)			

Table 2. IR spectroscopic data of selected Schiff base ligands and their Mo^{VI} complexes.[a]

Compd	$\tilde{\nu}$ [cm^{-1}]						
	(O–H)	(N–H)	(C=N)	(C=S/C=O)	(C–O)	$(Mo=O)_{asymm}$	$(Mo=O)_{symm}$
H_2L^1	3450*br*	3159*br*	1633*sh*	1210*m*	1271*m*	–	–
$MoO_2(L^1)$MeOH	3394*br*	3364*br*	1596*s*	–	1225*sh*	889*sh*	932*sh*
H_2L^2	3409*br*	3259*m*	1632*s*	1661*sh*	1121*sh*	–	–
$MoO_2(L^2)$MeOH	3500*br*	–	1605*sh*	–	1237*sh*	907*sh*	932*sh*
H_2L^3	3445*br*	3097*m*	1616*sh*	1032*sh*	1326*m*	–	–
$MoO_2(L^3)$MeOH	3337*br*	–	1591*sh*	–	1274*sh*	877*sh*	937*sh*

[a] *br*: broad, *sh*: sharp, *s*: strong, *m*: medium.

coordination.[22,24a,25] The absence of $\tilde{\nu}$(O–H) and $\tilde{\nu}$(N–H) in all the complexes indicates the ligands undergo deprotonation upon coordination. The existing $\tilde{\nu}$(O–H) and $\tilde{\nu}$(N–H) present in the complexes are attributed to the coordinated methanol molecule and the remaining NH group of the thiosemicarbazones. The two bands appearing at 877–907 cm^{-1} and 931–937 cm^{-1} are assigned to the asymmetric and symmetric Mo=O stretching vibrations and confirm the presence of the *cis*-MoO_2^{2+} moiety in the complex, consistent with similar Mo^{VI} complexes reported in the literature.[21d–e,24a,25,27]

Diffraction quality red–orange crystals of $[MoO_2(L^2)MeOH]$ (Figure 1a) and $[MoO_2(L^3)MeOH]$ (Figure 1b) were obtained following slow evaporation of methanolic solutions at room temperature or layering with pentane. The solid-state structures of the two complexes revealed that the ligands act as meridionally coordinating tridentate ONO and ONS donors. The crystal structure of the Mo^{VI} complex of H_2L^1 has been reported previously by the authors (CCDC 786365).[17] All three Mo^{VI} centres display distorted octahedral coordination geometry, consisting of the phenolate oxygen, imine nitrogen, and thio- or oxo-group donors from each Schiff base ligand, as well as two *cis*-dioxo ligands and a methanol solvent molecule. The *cis*-MoO_2^{2+} bond angles of H_2L^1 (104.91°), H_2L^2 (105.66°) and H_2L^3 (105.82°) and the average Mo=O bond length for the *cis*-MoO_2^{2+} of 1.70 Å are consistent with similar reported *cis*-dioxomolybdenum(VI) complexes.[21a,c,24,28] The O(2)–Mo–O(3) bond angle of 151.56° for the coordinated ligand oxygen atoms in $[MoO_2(L^2)MeOH]$ and the O(1)–Mo–S(1) bond angles of 152.25° and 151.26° in $[MoO_2(L^1)MeOH]$ and $MoO_2(L^3)MeOH]$, respectively, are consistent with literature values.[21c,29] Bond lengths and angles are summarised in Table 3. These three structurally characterised Mo^{VI} complexes highlight the potential of all three classes of Schiff bases to coordinate directly to a Mo^{VI} centre.

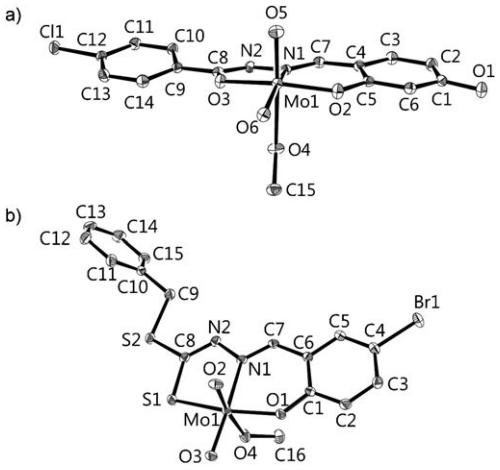

Figure 1. Ortep plots (50% probability ellipsoids) of the molecular structures of a) $[MoO_2(L^2)MeOH]$ and b) $[MoO_2(L^3)MeOH]$. Hydrogen atoms are omitted for clarity. Crystallographic data for these structures have been deposited with the Crystallographic Data Centre (deposition numbers: CCDC 809737, CCDC 809736).

Table 3. Selected bond lengths and angles for $[MoO_2(L^2)MeOH]$ and $[MoO_2(L^3)MeOH]$.

	$[MoO_2(L^2)MeOH]$		$[MoO_2(L^3)MeOH]$
Bond	[Å]	Bond	[Å]
Mo–O2	1.9287(10)	Mo-O1	1.9239(14)
Mo–O3	2.0124(10)	Mo-S1	2.4243(5)
Mo–O4	2.3601(12)	Mo-O4	2.3619(15)
Mo–O5	1.7094(12)	Mo-O2	1.6929(15)
Mo–O6	1.7044(10)	Mo-O3	1.7241(14)
Mo–N1	2.2301(12)	Mo-N1	2.2599(16)
N1–N2	1.4024(15)	N1-N2	1.401(2)
C7–N1	1.2940(18)	C7-N1	1.292(2)
Angle	(°)	Angle	(°)
O2–Mo–O3	151.56(4)	O1-Mo-S1	151.26(5)
O6–Mo–N1	155.01(5)	O3-Mo-N1	159.96(6)
O4–Mo–O5	172.13(4)	O2-Mo-O4	169.26(6)
O3–Mo–N1	71.77(4)	S1-Mo-N1	76.83(4)
O2–Mo–N1	81.94(4)	O1-Mo-N1	82.11(6)

[a] Values in brackets represent the estimated SD.

Biological screening

The XO inhibitory activity of each Schiff base was assessed spectrophotometrically by monitoring the formation of uric acid at 295 nm every minute for 10 min at 25 °C, according to the method employed by Bergmeyer et al. with minor modifications.[30] The reaction was initiated by the addition of XO (2.5 mU mL^{-1}) to a mixture of xanthine (50 μM) and the test compounds at various concentrations in 50 mM potassium dihydrogen orthophosphate buffer (pH 7.5). A negative control was carried out in the absence of test compounds, while allopurinol was used as a positive control and benchmark.

All inhibitors were dissolved in DMSO prior to introduction to the assay mixture, with the total DMSO concentration limited to 1% (*v*/*v*) in order to minimise the effect on XO activity. The percent inhibition at each inhibitor concentration was determined as reported in the literature.[31] The inhibitory perfor-

mance of each test compound was evaluated by its IC_{50} value, the concentration of inhibitor leading to a 50% decrease in the enzyme activity. This value was determined from sigmoidal plots of the inhibition versus log[inhibitor] for each test compound, given in Table 4 for the thiosemicarbazones, Table 5 for the hydrazones, and Table 6 for the dithiocarbazate Schiff bases. The positive control, allopurinol, gave an IC_{50} value of 3 ± 0 μM (mean ± standard deviation (SD), $n=2$) under the assay conditions employed, which is within the values reported in the literature.[2a]

Table 4. Inhibitory activity results for thiosemicarbazones.

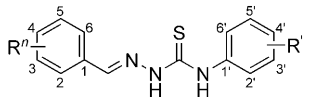

Compd	R^n	R′	Inhibition at 50 μM[a] [%]	IC_{50} [μM][a]
1a	2,4,6-OH	H	88±2	6±2
1b	2,4,6-OH	4′-Cl	95±1	1.8±0.1
1c	2,4,6-OH	4′-CN	89±1	0.6±0.2
1d	2,4,6-OH	3′-CN	80±0	6±0.2
2a	3-OH	H	92±0	4.7±0.2
2b	3-OH	4′-Cl	94±1	3.2±1.0
2c	3-OH	4′-CN	100±0	6.4±1.5
3a	2,4-OH	H	93±3	1.6±0.7
3b	2,4-OH	4′-Cl	95±4	0.5±0
3c	2,4-OH	4′-CN	96±1	0.6±0.1
4a	4-OH	H	95±1	1.3±0.1
4b	4-OH	4′-Cl	98±0	0.8±0.1
4c	4-OH	4′-CN	93±1	0.6±0
4d	4-OH	3′-CN	93±0	2.5±0.3
5a	4-OCH_3	H	7±1	–

[a] Values represent the mean ±SD of duplicate experiments.

The inhibitory activity of all compounds was initially tested at 50 μM concentrations. Compounds giving rise to a minimum of 50% inhibition were tested further at a range of concentrations in order to determine the IC_{50} value. Comparison of the inhibitory activity of the compounds in each class of Schiff bases, thiosemicarbazones, hydrazones and dithiocarbazates, allows SARs to be determined.

SAR analysis

In order to investigate the effect of the number and position of hydroxy substituents on inhibitory activity, thiosemicarbazones **1a**–**4a**, derived from different benzaldehydes (Scheme 2) but with the same unsubstituted thiosemicarbazide, were compared. The inhibitory performance appeared to increase in the order of **1a** < **2a** < **3a** ≈ **4a**. As the least potent compound bears three hydroxy substituents (**1a**) and the most potent bears one (**4a**), it can be concluded that the *position* is more significant than the *number* of hydroxy substituents for the inhibitory potencies of these Schiff base inhibitors. Compound series **3**, bearing a 2,4-dihydroxybenzaldehyde moiety, is more potent than compound series **1**, derived from 2,4,6-trihydroxybenzaldehyde, and series **4**, bearing 4-hydroxybenzaldehyde moiety, is generally more potent than series **3**, the hydroxy substituent in the *para*-position is again highlighted as being vital for potent activity. The important role that the substituent position has on activity is also confirmed on comparison of compounds **1b**–**4b** bearing *para*-chloro and **1c**–**4c** with *para*-cyano substituents on their thiosemicarbazide moiety, respectively. In general, the presence of a substituent (**b** and **c**) on the thiosemicarbazide ring of each Schiff base appears to improve the potency compared to their unsubstituted counterpart (**a**), for all benzaldehyde moieties (series **1**, **3**, **4**). Compounds derived from 3-hydroxybenzaldehyde (**2a**–**2c**), however, display statistically similar inhibitory activities, irrespective of the thiosemicarbazide used. On comparison of the *type* of aromatic substituent, compounds bearing the cyano substituent appear marginally more potent than their chloro counterparts (**1b** < **1c**, **4b** < **4c**).

To investigate whether a *meta*-cyano substituent would lead to increased potency, as seen in Y-700, febuxostat and Fyx-051, 3-cyanophenyl thiosemicarbazide was synthesised and condensed with 2,4,6-trihydroxybenzaldehyde (series **1**) and 4-hydroxybenzaldehyde (series **4**) to form Schiff bases **1d** and **4d**, respectively. On comparison of the inhibitory activity of these compounds with **1c** and **4c** bearing the cyano substituent in the *para*-position, it is evident that the *para* substituent is also important on the NH_2-bearing moiety of the Schiff base systems investigated. Additionally, in order to investigate whether the hydroxy substituent in compound **4a** acts as a hydrogen-bond donor, **5a** was synthesised, with a methoxy substituent in place of the hydroxy substituent. Analysis of the inhibitory activity of **5a** indicated a poor performance compared with **4a**, emphasising the need for hydrogen-bond donors. The hydroxy substituent in the *para*-position may be involved in stabilising the inhibitor in the enzyme active site through the formation of hydrogen bonds with neighbouring amino acid residues. Under the assay conditions employed, thiosemicarbazones **1b**, **1c**, **3a**, **3b**, **3c**, **4a**, **4b** and **4c** gave IC_{50} values lower than the benchmark allopurinol, with **1c**, **3b**, **3c**, **4b** and **4c** displaying approximately four-times increased potency. The common substituents in these promising Schiff bases are a hydroxy substituent in the *para*-position of the benzaldehyde moiety and a *para* substituent, either chloro or cyano, on the thiosemicarbazide aromatic ring.

Upon inhibitory activity testing of hydrazones **1e**–**4e**, they were found to be less potent than the thiosemicarbazones. This can be attributed to the presence of an additional NH group in the thiosemicarbazones, which can lead to improved stabilisation through formation of hydrogen bonds with key amino acids residues. In addition, the presence of a sulfur in place of the more electronegative oxygen seen in the hydrazones, may play a role in the improved potency of the thiosemicarbazones, owing to the thiophilic nature of the Mo centre in the active site. Hydrazones of series **1**, **2**, **3** and **4** were synthesised (Table 5). Initial activity testing at 50 μM gave rise to ≥50% inhibition for series **1** hydrazones, but revealed poor inhibitory performance (≈15% inhibition) for hydrazones of benzaldehyde moieties with fewer hydroxy substituents. The presence of multiple hydroxy substituents can lead to a great-

Table 5. Inhibitory activity results for hydrazones.

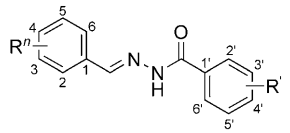

Compd	R^n	R′	Inhibition at 50 μM[a] [%]	IC_{50} [μM][a]
1e	2,4,6-OH	4′-OH	96±4	19±0
1f	2,4,6-OH	4′-Br	71±4	32±1
1g	2,4,6-OH	4′-Cl	59±2	63±1
1h	2,4,6-OH	3′-OH	60±2	74±3
1i	2,4,6-OH	3′-Br	64±3	55±5
1j	2,4,6-OH	3′-Cl	61±1	48±6
1k	2,4,6-OH	2′-OH	41±9	85±12
2d	3-OH	4′-OH	17±1	–
2e	3-OH	4′-Br	16±0	–
2f	3-OH	4′-Cl	14±0	–
3d	2,4-OH	4′-OH	26±1	–
3e	2,4-OH	4′-Br	12±4	–
3f	2,4-OH	4′-Cl	8±3	–
4e	4-OH	4′-OH	13±0	–

[a] Values represent the mean ±SD of duplicate experiments.

er number of stabilising polar interactions as well as improved solubility. As a consequence of the low inhibition, IC_{50} values were not determined for hydrazones **2d**–**4e**. Analysis of the IC_{50} values for the 2,4,6-trihydroxybenzaldehyde hydrazones revealed interesting trends in the substitution pattern of the hydrazide moiety. The activity of compounds differing only in the *position* of the hydroxy substituent on the hydrazide moiety decreases in the order of **1e** (*p*-OH) >**1h** (*m*-OH) >**1k** (*o*-OH). The trend is also repeated for bromo -substituted compounds as **1f** (*p*-Br) >**1i** (*m*-Br). This again emphasises the *para*-position of aromatic substituents on the hydrazide ring as being vital for potent inhibition. In terms of the *type* of the substituent, as the inhibitory activity increased in the order of **1g** (*p*-Cl) <**1f** (*p*-Br) <**1e** (*p*-OH), the hydroxy substituent was again highlighted as an important substituent for potent inhibition, in line with previous studies on flavonoids.[13,14] The trend was, however, reversed when the *meta*-substituted hydrazones were considered, with the inhibitory activity increasing in the order of **1h** (*m*-OH) <**1i** (*m*-Br) <**1j** (*m*-Cl). This indicates that both the *position* and the *type* of substituent greatly influences inhibitory activity and reinforces the aforementioned findings for the thiosemicarbazones.

From the improved performance of the thiosemicarbazone- over the hydrazone-type Schiff bases, it is evident that the presence of a sulfur atom in place of an oxygen atom plays a significant role in inhibition. It was, therefore, hypothesised that the presence of two sulfur atoms may lead to improved potency. *S*-Benzyldithiocarbazate was, therefore, condensed with a range of hydroxy-substituted benzaldehydes (Table 6) in order to investigate effects on inhibition. Determination of the inhibitory activities of compounds **1l**, **3g**, **4f**, **6a** was undertaken. As the order of potency increased on going from **1l** < **3g** <**4f**, it appeared that the activity increased as the number of hydroxy substituents decreased, as seen previously with the thiosemicarbazones. The presence of a hydroxy substituent in

Table 6. Inhibitory activity results for dithiocarbazates.

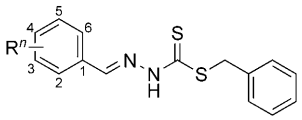

Compd	R^n	Inhibition at 50 μM[a] [%]	IC_{50} [μM][a]
1l	2,4,6-OH	74±5	12±3
3g	2,4-OH	87±3	5±1
4f	4-OH	95±4	0.7±0.1
6a	2-OH, 5-Br	40±2	–

[a] Values represent the mean ±SD of duplicate experiments.

the *para*-position of the benzaldehyde moiety led to the most potent compound of the dithiocarbazate class, with **4f** being approximately four-times more potent than allopurinol under the assay conditions employed. On comparison of the dithiocarbazates **1l** and **3g**, and the unsubstituted thiosemicarbazone counterparts **1a** and **3a**, the presence of a second sulfur atom does not appear to lead to improved potency. In contrast, for 4-hydroxybenzaldehyde Schiff bases, the dithiocarbazate **4f** gave a lower IC_{50} value than its thiosemicarbazone counterpart **4a**. Co-crystallisation studies are, therefore, required to explain this deviation from the trend, hypothesised to be attributed to the location and number of polar interactions between inhibitors and the amino acids in the narrow channel of the active site.

Steady-state kinetics

The mode of inhibition of potent Schiff bases was investigated using Lineweaver–Burk plots. In these steady-state kinetic studies, the rate of the reaction was monitored as the concentration of the inhibitor and the substrate, xanthine, were varied. As reported previously, the in vitro investigation of the mode of inhibition for **1c**, revealed a mixed-type inhibitory behaviour, with a K_i value of 0.7±0.2 μM and K'_i value of 1.4± 0.1 μM.[17] Compounds **4c** and **4f** displayed the same mode of inhibition (Table 7). From this observation, it can be deduced that both the thiosemicarbazones **1c** and **4c** and the dithiocarbazate **4f** inhibit the enzyme by blocking the narrow channel leading to the molybdopterin active site. The mixed-type inhibition is in accordance with the majority of nonpurine inhibitors reported in the literature, such as Y-700 and febuxo-

Table 7. Mode of inhibition (MoI) data.

Compd	MoI	V_{max} [AU min^{-1}]	K_m [μM]	K_i [μM][a]	K'_i [μM][a]
1c	Mixed-type	Decreases (0.023–0.013)	Increases (8.93–12.16)	0.7±0.2	1.4±0.1
4c	Mixed-type	Decreases (0.032–0.021)	Increases (12.76–19.32)	1.1±0.9	2.4±1.6
4f	Mixed-type	Decreases (0.032–0.014)	Increases (18.83–27.90)	0.4±0.0	0.8±0.2

[a] Values represent the mean ±SD of duplicate experiments.

stat. Co-crystallisation studies of these inhibitors with XO reported in the literature revealed that they are held in place by a number of polar and nonpolar interactions with neighbouring amino acid residues.[6, 9a, 20]

Copper(II) complexation studies

The use of transition metal complexes with similar ONS and ONO donor Schiff base ligands as novel XO inhibitors has been reported in the literature by Zhu et al.[18a–c] In their studies, Cu^{II} complexes displayed XO inhibitory activities comparable to allopurinol. Further research into the use of transition metals as inhibitors of the enzyme revealed that copper salts can independently inhibit XO.[32] In order to investigate the potential of increased potency on complexation to copper, thiosemicarbazone **3b** and hydrazone **1i** were used in preparation of the respective copper(II) complexes (Scheme 4).

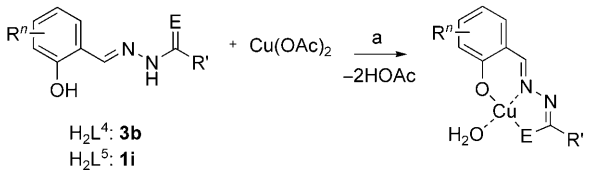

H_2L^4: **3b**
H_2L^5: **1i**

Scheme 4. Synthesis of Cu^{II} complexes of thiosemicarbazone **3b** and hydrazone **1i** ligands. *Reagent and conditions*: a) copper–ligand ratio 1:1, methanol, reflux, 53–80%.

Evidence of complexation was obtained by UV/vis spectroscopy, IR spectroscopy and elemental analysis. From the characterisation data obtained, it can be concluded that the ligands behave as tridentate ONO/ONS donors, with chelating phenolate oxygen, imine nitrogen, and thio or oxo donors, in accordance to similar reported complexes.[33] The presence of water was determined by elemental analysis. The complexes were insoluble in methanol, ethanol and acetone, but readily soluble in DMSO. On analysis of the inhibitory activities of the complexes, the IC_{50} values (Table 8) were approximately three-times lower than their corresponding free ligands. The improved potency of the copper(II) complexes mirrors the findings reported by Zhu et al.[18a–b]

Although the role of copper in XO inhibition is still under investigation, several potential modes of action have been proposed. Steady-state kinetic studies have revealed the noncompetitive nature of inhibition of Cu^{II} salts, ruling out direct coordination to the Mo^{VI} active site.[34] A study by Mondal et al. revealed that the oxidative half reaction, catalysed by XO, is affected during Cu^{II} inhibition, indicating interruption of the process occurring at the FAD cofactor, where molecular oxygen is used as the final electron acceptor. Inhibition may, therefore, occur as a result of slower reoxidation of Mo^{IV} to its active Mo^{VI} form. A more recent study by Sau et al. reports evidence for the direct coordination of the Cu^{II} to XO via sulfur or nitrogen ligands.[34b, 35] These ligands can arise from amino acids, such as cysteine, surrounding the FAD. An alternative hypothesis involves the formation of deleterious hydroxy radicals produced in the Haber–Weiss reaction, catalysed by Cu^{II}.[36] Although the exact mechanism of inhibition is unknown, is it evident that there exists an additive effect in having a Schiff base ligand and a Cu^{II} present, leading to greater inhibitory activity.

Table 8. XO inhibitory activity results for Schiff bases **1i** and **3b** and their Cu^{II} complexes.[a]

	IC_{50} [μM]	
	3b	**1i**
Free ligand	0.5 ± 0	55 ± 5
Copper complex	0.2 ± 0	16 ± 3

[a] Values represent the mean ± SD of duplicate experiments.

Conclusions

The synthesis, characterisation, and XO inhibitory activity of Schiff bases derived from a series of benzaldehydes and three classes of NH_2-containing aromatic compounds was undertaken. In particular, the *number* and *position* of hydroxy substituents on the benzaldehyde moiety was investigated. Schiff base ligands from each class— thiosemicarbazone, hydrazone and dithiocarbazate—readily formed Mo^{VI} complexes upon reaction with $[MoO_2(acac)_2]$. This highlights the potential of direct attachment or close association with the molybdo(VI)-pterin in the enzyme active site. On testing, thiosemicarbazones **1c**, **3b**, **3c**, **4b** and **4c** and dithiocarbazate **4f** displayed significantly increased potency over the benchmark allopurinol under the employed assay conditions. The SAR study performed on thiosemicarbazones, hydrazones and dithiocarbazates revealed that the *position* rather than the *number* of hydroxy substituents is important for potent XO inhibition.

A hydroxy substituent in the *para*-position on the benzaldehyde unit gave rise to the most potent Schiff bases. In addition, the presence of chloro and cyano substituents in the *para*-position of the aromatic ring of the thiosemicarbazide unit led to increased potency over the unsubstituted counterparts. Having a substituent in the *para*-position of aryl hydrazides was also significant for potent XO inhibition in hydrazones, with the hydroxy substituent giving rise to improved inhibition. Substitution of the hydroxy with a methoxy substituent led to a dramatic loss of activity, indicating the need for hydrogen-bond donor substituents. Groups such as OH, NH and CN are postulated to contribute to stabilising polar interactions between the inhibitors and amino acid residues in the access channel of the enzyme. Oxygen-containing hydrazones were less potent than sulfur-containing Schiff bases, highlighting the importance of sulfur for potent XO inhibitory activity. In addition, steady-state kinetic studies revealed mixed-type inhibition for both thiosemicarbazone and dithiocarbazate Schiff bases. The definitive mode of inhibition and the number and type of stabilising interactions holding these Schiff base inhibitors in place will be determined from co-crystallisation studies with XO. The initial testing of Cu^{II} complexes versus their free ligands revealed a threefold improvement in inhibition, which will be investigated further.

Experimental Section

Materials and instrumentation: 2,4,6-Trihydroxybenzaldehyde, 2,4-dihydroxybenzaldehyde, 3-hydroxybenzaldehyde, 4-hydroxybenzaldehyde, 4-methoxybenzaldehyde, 5-bromo-2-hydroxybenzaldehyde, 4-phenyl-3-thiosemicarbazide, aryl hydrazides and [D_6]DMSO were purchased from Aldrich. Xanthine oxidase and allopurinol were purchased from Sigma. Potassium dihydrogen orthophosphate used in the enzyme assays was purchased from Fisher Chemicals and reagent grade DMSO and was purchased from Fisher Scientific. 4-(4-Chlorophenyl)-3-thiosemicarbazide was purchased from Alfa Aesar. All reagents were used as supplied. 4-(4-Cyanophenyl)-3-thiosemicarbazide and 4-(3-cyanophenyl)-3-thiosemicarbazide were synthesised by refluxing $N_2H_4{\cdot}H_2O$ (Sigma–Aldrich) with equimolar amounts of 4-cyanophenyl isothiocyanate (Alfa Aesar) and 3-cyanophenyl isothiocyanate (Aldrich) respectively. *S*-Benzyldithiocarbazate was synthesised as previously reported.[37] ^{1}H and ^{13}C {^{1}H}-decoupled NMR spectra were recorded on a Jeol EX and ES 400 instrument (^{1}H NMR 400 MHz; ^{13}C NMR 100 MHz). Assignment of resonances was confirmed by HSQC spectra. Multiplicity abbreviations are reported as follows: s = singlet; bs = broad singlet; d = doublet; t = triplet; dd = double doublet; m = multiplet; q = quartet. Infrared (IR) spectra were recorded on a Thermo Nicolet Avatar 370 FTIR spectrophotometer in the region of 4000–400 cm^{-1}: br = broad; sh = sharp; s = strong; m = medium; w = weak. Melting points were measured on a Stuart Scientific SMP3 apparatus. Elemental analysis of compounds was carried out on an Exeter CE-440 elemental analyser and are within ±0.4% of the calculated value. Electrospray ionisation mass spectrometry (ESI-MS) and high resolution mass spectra (HRMS) were recorded on a Bruker microTOF electrospray mass spectrometer. Xanthine oxidase inhibitory activity assays were carried out using a Jenway 6705 UV/vis spectrophotometer with thermostated cell holder. Diffraction data was collected on a Bruker Smart Apex diffractometer at 110 K with Mo Kα radiation (λ = 0.71073 Å).

General procedure for Schiff base synthesis: A solution of the appropriate benzaldehyde (1 mmol) in EtOH (10 mL) was treated with the appropriate thiosemicarbazide, hydrazide or dithiocarbazate (1 mmol), and the resulting mixture was refluxed for 4 h. The precipitate that formed after partial evaporation of the solvent or by addition of a minimum amount of water was isolated, washed with EtOH and dried. The products obtained were isolated in yields of 40–95%. Characterisation data for compounds **1a**–**1c**, **1e**–**1k** and [MoO_2(L^1)MeOH] can be found elsewhere.[17]

1-(3-Cyanophenyl)-3-[(2,4,6-trihydroxyphenyl)methylidene]amino thiourea (1d): Pale orange solid (58 mg, 0.18 mmol, 70%): R_f = 0.43 (MeOH/$CHCl_3$ 1:8); mp: 199–200 °C (dec); ^{1}H NMR (400 MHz, [D_6]DMSO): δ = 5.84 (s, 2H), 7.54 (t, 1H, J = 8.0 Hz), 7.61 (d, 1H, J = 7.4 Hz), 7.85 (d, 1H, J = 7.8 Hz), 8.00 (s, 1H), 8.60 (s, 1H, C*H*N), 9.91 (s, 1H, O*H*/N*H*), 10.02 (s, 1H, O*H*/N*H*), 10.12 (s, 1H, O*H*/N*H*), 11.74 ppm (s, 1H, O*H*/N*H*); ^{13}C{^{1}H} NMR (100 MHz, [D_6]DMSO): δ = 94.7, 99.0, 110.8 (4C_{ar}), 118.7, 128.5, 129.5, 130.4, 140.6, 145.2 (*C*HN), 155.9, 159.4, 161.9 ppm (*C*=S); FTIR (KBr): $\tilde{\nu}_{max}$ = 3335 (O–H, sh), 3253 (N–H, sh), 2245 (C≡N, sh), 1643 (C=N, sh, m), 1550 (C=C, sh, m), 1263 (C–O, m), 1050 cm^{-1} (C=S, sh); HRMS (ESI): m/z [M+H]$^+$ calcd for $C_{15}H_{13}N_4O_3S$: 329.0703, found: 329.0706 (difference = −0.3 mDa); Anal. calcd for $C_{15}H_{12}N_4O_3S{\cdot}1.01\,H_2O$: C 51.99, H 4.08, N 16.17, found: C 51.98, H 4.05, N 16.73.

(2,4,6-Trihydroxybenzaldehyde)dithiocarbazate (1l): Pale orange solid (0.27 g, 0.81 mmol, 80%): R_f = 0.57 (MeOH/$CHCl_3$ 1:8); mp: 184–185 °C; ^{1}H NMR (400 MHz, [D_6]DMSO): δ = 4.53 (s, 2H, CH_2), 5.84 (s, 2H), 7.27 (t, 1H, J = 7.4 Hz), 7.33 (t, 2H, J = 7.0 Hz), 7.41 (d, 2H, J = 7.0 Hz), 8.65 (s, 1H, C*H*N), 10.05 (s, 1H, O*H*), 10.50 ppm (s, 2H, O*H*/N*H*); ^{13}C{^{1}H} NMR (100 MHz, [D_6]DMSO): δ = 39.2 (CH_2), 95.8, 100.1, 128.2, 129.4, 130.2, 137.7, 146.7 (*C*HN), 161.2 (4C_{ar}), 163.5 (4C_{ar}), 195.0 ppm (*C*=S); FTIR (KBr): $\tilde{\nu}_{max}$ = 3392 (O–H, br), 3200 (N–H, br), 3099 (C–H_{ar}, w), 2969 (C–H_{alkyl}, w), 1634 (C=N, sh), 1583 (C=C, sh), 1293 (C–O, sh, s), 1029 cm^{-1} (C=S, sh); UV/vis (DMSO): λ_{max} (ε) = 295 (8203), 368 (27496), 384 nm (23772); HRMS (ESI): m/z [M+H]$^+$ calcd for $C_{15}H_{15}N_2O_3S_2$: 335.0513, found: 335.0519 (difference = 0.5 mDa); Anal. calcd for $C_{15}H_{14}N_2O_3S_2{\cdot}1\,H_2O$: C 51.13, H 4.58, N 7.96, found: C 50.77, H 4.51, N 7.87.

3-[(3-Hydroxyphenyl)methylidene]amino-1-phenylthiourea (2a): Pale yellow crystalline solid (0.11 g, 0.39 mmol, 77%): R_f = 0.70 (MeOH/Et_2O 1:10); mp: 202–203 °C (lit. 194 °C);[38] ^{1}H NMR (400 MHz, [D_6]DMSO): δ = 6.81 (1H, dd, J = 7.8, 1.3 Hz), 7.16–7.35 (6H, m), 7.55 (2H, d, J = 7.5 Hz), 8.05 (1H, s, C*H*N), 9.53 (1H, bs, O*H*/N*H*), 11.74 ppm (1H, bs, O*H*/N*H*); ^{13}C{^{1}H} NMR (100 MHz, [D_6]DMSO): δ = 113.8, 117.3, 118.9, 125.3, 125.8, 128.1, 129.7, 135.3, 139.1, 143.2 (*C*HN), 157.6 (4C_{ar}), 175.9 ppm (*C*=S); FTIR (KBr): $\tilde{\nu}_{max}$ = 3394 (O–H, br), 3311 (N–H, sh, m), 3172 (C–H_{ar}, w), 1581 (C=N, sh, m), 1546, 1510 (C=C, sh, s), 1287 (C–O, sh, s), 1165 cm^{-1} (C=S, sh); HRMS (ESI): m/z [M+H]$^+$ calcd for $C_{14}H_{13}N_3OS$: 272.0852, found: 272.0852 (difference = −0.3 mDa); Anal. calcd for $C_{14}H_{13}N_3OS$: C 61.97, H 4.83, N 15.49, found: C 61.71, H 4.88, N 15.76.

1-(4-Chlorophenyl)-3-[(3-hydroxyphenyl)methylidene]amino-thiourea (2b): Beige solid (97 mg, 0.32 mmol, 65%): R_f = 0.70 (MeOH/Et_2O 1:10); mp: 207–208 °C; ^{1}H NMR (400 MHz, [D_6]DMSO): δ = 6.83 (dd, 1H, J = 8.5, 2.0 Hz), 7.22 (t, 1H, J = 7.0 Hz), 7.26–7.30 (m, 2H), 7.41 (d, 2H, J = 8.5 Hz), 7.61 (d, 2H, J = 8.5 Hz), 8.07 (s, 1H, C*H*N), 9.57 (bs, 1H, O*H*/N*H*), 10.13 (bs, 1H, O*H*/N*H*), 11.85 ppm (bs, 1H, N*H*); ^{13}C{^{1}H} NMR (100 MHz, [D_6]DMSO): δ = 113.9, 117.4, 119.0, 127.5, 128.0, 129.3, 129.7, 135.2, 138.1, 143.6 (*C*HN), 157.6 (4C_{ar}), 176.0 ppm (*C*=S); FTIR (KBr): $\tilde{\nu}_{max}$ = 3400 (O–H, br), 3281 (N–H, br), 1591 (C=N, sh, m), 1550, 1490 (C=C, sh), 1276 (C–O, sh, m), 1197 cm^{-1} (C=S, sh); HRMS (ESI): m/z [M+H]$^+$ calcd for $C_{14}H_{13}N_3OSCl$: 306.0462, found: 306.0457 (difference = 0.9 mDa); Anal. calcd for $C_{14}H_{12}N_3OSCl{\cdot}0.3\,H_2O$: C 54.04, H 4.08, N 13.50, found: C 53.92, H 3.95, N 14.05.

1-(4-Cyanophenyl)-3-[(3-hydroxyphenyl)methylidene]amino-thiourea (2c): Pale yellow solid (33 mg, 0.11 mmol, 62%): R_f = 0.52 (MeOH/$CHCl_3$ 1:8); mp: 197–198 °C; ^{1}H NMR (400 MHz, [D_6]DMSO): δ = 6.82 (bd, 1H, J = 8.5 Hz), 7.23 (t, 1H, J = 8.0 Hz), 7.26–7.30 (m, 2H), 7.81 (d, 2H, J = 8.8 Hz), 7.94 (bd, 2H, J = 8.8 Hz), 8.10 (s, 1H, C*H*N), 9.61 (bs, 1H, O*H*/N*H*), 10.28 (bs, 1H, O*H*/N*H*), 12.02 ppm (bs, 1H, N*H*); ^{13}C{^{1}H} NMR (100 MHz, [D_6]DMSO): δ = 106.8, 113.8, 117.4, 118.9, 119.0, 124.8, 129.6, 132.1, 134.9, 143.4, 144.1 (*C*HN), 157.5 (4C_{ar}), 175.2 ppm (*C*=S); FTIR (KBr): $\tilde{\nu}_{max}$ = 3389 (O–H, m), 3296 (N–H, sh, m), 2235 (C≡N, sh), 1606 (C=N, sh), 1583 (C=C, sh), 1276 (C–O, sh), 1203 cm^{-1} (C=S, sh); HRMS (ESI): m/z [M+H]$^+$ calcd for $C_{15}H_{13}N_4OS$: 297.0805, found: 297.0806 (difference = −0.1 mDa); Anal. calcd for $C_{15}H_{12}N_4OS$: C 60.79, H 4.08, N 18.91, found: C 60.62, H 4.08, N 19.25.

4-Hydroxy-*N*′-[(3-hydroxyphenyl)methylidene]benzohydrazide (2d): White crystalline solid (81 mg, 0.32 mmol, 63%): R_f = 0.47 (MeOH/Et_2O 1:10); mp: >250 °C (dec) (lit. 271 °C);[39] ^{1}H NMR (400 MHz, [D_6]DMSO): δ = 6.82 (dd, 1H, J = 8.0, 2.0 Hz), 6.84 (d, 2H, J = 8.4 Hz), 7.08 (d, 1H, J = 7.6 Hz), 7.19 (bs, 1H), 7.24 (t, 1H, J = 7.8 Hz), 7.80 (d, 2H, J = 8.5 Hz), 8.33 (s, 1H, C*H*N), 9.85 (bs, 1H, O*H*), 11.59 ppm (bs, 1H, N*H*); ^{13}C{^{1}H} NMR (100 MHz, [D_6]DMSO): δ = 112.5, 115.1, 117.3, 118.7, 124.2, 129.7, 129.9, 135.8, 147.1 (*C*HN), 157.7 (4C_{ar}), 161.2 (4C_{ar}), 162.6 ppm (*C*=O); FTIR (KBr): $\tilde{\nu}_{max}$ = 3455 (O–H, br), 3233 (N–H, br), 1628 (C=O, sh, m), 1587 (C=N, sh, m),

1508 (C=C, sh), 1240 (C–O, sh), 1168 cm^{-1} (C–O, sh); HRMS (ESI): *m/z* $[M+H]^+$ calcd for $C_{14}H_{13}N_2O_3$: 257.0921, found: 257.0921 (difference = 0.0 mDa); Anal. calcd for $C_{14}H_{12}N_2O_3 \cdot 1H_2O$: C 61.31, H 5.14, N 10.21, found: C 61.05, H 5.12, N 10.28.

4-Bromo-*N*′-[(3-hydroxyphenyl)methylidene]benzohydrazide (2e): White solid (0.14 g, 0.43 mmol, 87%): R_f = 0.63 (MeOH/Et_2O 1:10); mp: >250 °C (dec); ^{1}H NMR (400 MHz, [D_6]DMSO): δ = 6.84 (dd, 1H, *J* = 8.0, 2.0 Hz), 7.10 (d, 1H, *J* = 7.5 Hz), 7.21 (s, 1H), 7.26 (t, 1H, *J* = 7.5 Hz), 7.74 (d, 2H, *J* = 8.5 Hz), 7.86 (d, 2H, *J* = 8.5 Hz), 8.35 (s, 1H, C*H*N), 9.64 (bs, 1H, O*H*), 11.86 ppm (bs, 1H, N*H*); ^{13}C{^{1}H} NMR (100 MHz, [D_6]DMSO): δ = 112.6, 117.6, 118.9, 125.6, 129.7, 129.9, 131.5, 132.5, 135.5, 148.3 (*C*HN), 157.7 ($4C_{ar}$), 162.2 ppm (*C*=O); FTIR (KBr): $\tilde{\nu}_{max}$ = 3487 (O–H, br), 3308 (N–H, br), 1665 (C=O, s), 1578 (C=N, sh), 1483 (C=C, sh), 1288 cm^{-1} (C–O, s); HRMS (ESI): *m/z* $[M]^+$ calcd for $C_{14}H_{11}N_2O_2Br$: 319.0077, found: 319.0070 (difference = 0.7 mDa); Anal. calcd for $C_{14}H_{11}N_2O_2Br \cdot 0.49H_2O$: C 51.27, H 3.68, N 8.54, found: C 51.27, H 3.71, N 8.11.

4-Chloro-*N*′-[(3-hydroxyphenyl)methylidene]benzohydrazide (2f): White solid (70 mg, 0.26 mmol, 51%): R_f = 0.63 (MeOH/Et_2O 1:10); mp: 219–220 °C; ^{1}H NMR (400 MHz, [D_6]DMSO): δ = 6.81 (dd, 1H, *J* = 8.0, 1.6 Hz), 7.11 (d, 1H, *J* = 7.6 Hz), 7.21 (s, 1H), 7.26 (t, 1H, *J* = 7.6 Hz), 7.61 (d, 2H, *J* = 8.4 Hz), 7.94 (d, 2H, *J* = 8.4 Hz), 8.35 (s, 1H, C*H*N), 9.64 (bs, 1H, O*H*), 11.90 ppm (bs, 1H, N*H*); ^{13}C{^{1}H} NMR (100 MHz, [D_6]DMSO): δ = 112.6, 117.6, 118.9, 128.6, 129.6, 130.0, 132.2, 135.5, 136.6, 148.2 (*C*HN), 157.7 ($4C_{ar}$), 162.0 ppm (*C*=O); FTIR (KBr): $\tilde{\nu}_{max}$ = 3406 (O–H, br), 3227 (N–H, br), 1645 (C=O, sh), 1595 (C=N, sh), 1489 (C=C, sh), 1288 cm^{-1} (C–O, sh); HRMS (ESI): *m/z* $[M+H]^+$ calcd for $C_{14}H_{12}N_2O_2Cl$: 275.0582, found: 275.0587 (difference = −0.5 mDa); Anal. calcd for $C_{14}H_{11}N_2O_2Cl \cdot 1.61H_2O$: C 55.37, H 4.72, N 9.22, found: C 55.39, H 4.56, N 9.07.

3-[(2,4-Dihydroxyphenyl)methylidene]amino-1-phenylthiourea (3a): Yellow solid (78 mg, 0.27 mmol, 54%): R_f = 0.58 (MeOH/Et_2O 1:10); mp: >200 °C (dec); ^{1}H NMR (400 MHz, [D_6]DMSO): δ = 6.29 (dd, 1H, *J* = 8.8, 2.4 Hz), 6.32 (d, 1H, *J* = 2.4 Hz), 7.17 (t, 1H, *J* = 7.5 Hz), 7.34 (t, 2H, *J* = 7.7 Hz), 7.57 (d, 2H, *J* = 7.6 Hz), 7.87 (d, 1H, *J* = 8.5 Hz), 8.36 (s, 1H, C*H*N), 9.81 (bs, 1H, O*H*/N*H*), 9.85 (s, 1H, O*H*/N*H*), 9.91 (bs, 1H, O*H*/N*H*), 11.59 ppm (bs, 1H, N*H*); ^{13}C{^{1}H} NMR (100 MHz, [D_6]DMSO): δ = 102.3, 107.8, 111.8, 125.0, 125.5, 128.0, 128.6, 139.3, 140.8 (*C*HN), 158.3 ($4C_{ar}$), 160.7 ($4C_{ar}$), 174.9 ppm (*C*=S); FTIR (KBr): $\tilde{\nu}_{max}$ = 3400 (O–H, br), 3141 (N–H, br), 1610 (C=N, s), 1545 (C=C, m), 1214 (C–O, m), 1121 cm^{-1} (C=S, sh, s); HRMS (ESI): *m/z* $[M+H]^+$ calcd for $C_{14}H_{14}N_3O_2S$: 288.0801, found: 288.0797 (difference = 0.4 mDa); Anal. calcd for $C_{14}H_{13}N_3O_2S \cdot 0.69H_2O$: C 56.09, H 4.84, N 14.02, found: C 56.08, H 4.74, N 14.28.

1-(4-Chlorophenyl)-3-[(2,4-dihydroxyphenyl)methylidene]amino-thiourea (3b): Yellow solid (0.11 g, 0.35 mmol, 54%): R_f = 0.55 (MeOH/$CHCl_3$ 1:8); mp: >200 °C (dec); ^{1}H NMR (400 MHz, [D_6]DMSO): δ = 6.30 (dd, 1H, *J* = 7.0, 2.0 Hz), 6.31 (d, 1H, *J* = 2.0 Hz), 7.38 (d, 2H, *J* = 8.8 Hz), 7.60 (d, 2H, *J* = 8.8 Hz), 7.86 (d, 1H, *J* = 7.0 Hz), 8.36 (s, 1H, C*H*N), 9.82 (bs, 1H, O*H*), 9.87 (bs, 1H, O*H*), 9.96 (bs, 1H, N*H*), 11.66 (bs, 1H, N*H*); ^{13}C{^{1}H} NMR (100 MHz, [D_6]DMSO): δ = 102.3, 107.8, 111.7 ($4C_{ar}$), 127.1, 127.9, 128.3, 128.9, 138.3, 142.2 (*C*HN), 158.3 ($4C_{ar}$), 160.8 ($4C_{ar}$), 174.5 ppm (*C*=S); FTIR (KBr): $\tilde{\nu}_{max}$ = 3450 (O–H, br), 3159 (N–H, br), 1633 (C=N, s, sh), 1547 (C=C, s), 1271 (C–O, m), 1210 cm^{-1} (C=S, m); UV/vis (DMSO): λ_{max} (ε) = 293 (14482), 308 (15190), 350 nm (30722); HRMS (ESI): *m/z* $[M+H]^+$ calcd for $C_{14}H_{13}N_3O_2SCl$: 322.0412, found: 322.0407 (difference = 0.5 mDa); Anal. calcd for $C_{14}H_{12}N_3O_2SCl \cdot 0.39H_2O$: C 51.15, H 3.92, N 12.78, found: C 51.17, H 3.93, N 12.59.

1-(4-Cyanophenyl)-3-[(2,4-dihydroxyphenyl)methylidene]amino-thiourea (3c): Yellow solid (51 mg, 0.16 mmol, 65%): R_f = 0.18 (MeOH/$CHCl_3$ 1:4); mp: >250 °C (dec); ^{1}H NMR (400 MHz, [D_6]DMSO): δ = 6.29 (1H, bd, *J* = 1.8 Hz), 6.31 (1H, bd), 7.80 (2H, d, *J* = 8.6 Hz), 7.88 (1H, bd, *J* = 8.2 Hz), 7.97 (2H, d, *J* = 8.6 Hz), 8.40 (1H, s, C*H*N), 9.85 (1H, bs, O*H*/N*H*), 9.90 (1H, bs, O*H*/N*H*), 10.14 (1H, bs, O*H*/N*H*), 11.87 ppm (1H, s, N*H*); ^{13}C{^{1}H} NMR (100 MHz, [D_6]DMSO): δ = 102.3, 106.1, 107.7, 111.4, 118.9, 124.4, 128.4, 132.1, 141.6, 143.5 (*C*HN), 158.3 ($4C_{ar}$), 160.8 ($4C_{ar}$), 174.1 ppm (*C*=S); FTIR (KBr): $\tilde{\nu}_{max}$ = 3360 (O–H, m), 3299 (N–H, m), 3164 (C–H_{ar}, w), 2236 (C≡N, sh, m), 1633 (C=N, sh), 1550, 1514 (C=C, sh), 1238, 1214 (C–O, sh), 1127 cm^{-1} (C=S, sh); HRMS (ESI): *m/z* $[M+H]^+$ calcd for $C_{15}H_{13}N_4O_2S$:313.0754, found: 313.0750 (difference = 0.4 mDa); Anal. calcd for $C_{15}H_{12}N_4O_2S$: C 57.68, H 3.87, N 17.94, found: C 57.47, H 3.91, N 18.37.

***N*′-[(2,4-Dihydroxyphenyl)methylidene]-4-hydroxybenzohydrazide (3d)**: Beige solid (54 mg, 0.20 mmol, 40%): R_f = 0.37 (MeOH/Et_2O 1:10); mp: >250 °C (dec); ^{1}H NMR (400 MHz, [D_6]DMSO): δ = 6.30 (s, 1H), 6.34 (d, 1H, *J* = 8.0 Hz), 6.85 (d, 2H, *J* = 8.5 Hz), 7.26 (d, 1H, *J* = 8.0 Hz), 7.79 (d, 2H, *J* = 8.5 Hz), 8.45 (s, 1H, C*H*N), 10.05 (bs, 2H, O*H*), 11.59 (bs, 1H, O*H*/N*H*), 11.72 ppm (bs, 1H, O*H*/N*H*); ^{13}C{^{1}H} NMR (100 MHz, [D_6]DMSO): δ = 102.7, 107.6, 110.6, 115.1, 123.3, 129.6, 131.4, 148.5 (*C*HN), 159.5 ($4C_{ar}$), 160.5 ($4C_{ar}$), 160.9 ($4C_{ar}$), 162.2 ppm (*C*=O); FTIR (KBr): $\tilde{\nu}_{max}$ = 3348 (O–H, m), 3150 (N–H, br), 1650 (C=O, sh), 1633 (C=N, sh), 1603 (C=C, sh), 1259, 1175 cm^{-1} (C–O, sh); HRMS (ESI): *m/z* $[M+H]^+$ calcd for $C_{14}H_{13}N_2O_4$ 273.0870, found: 273.0873 (difference = −0.4 mDa); Anal. calcd for $C_{14}H_{12}N_2O_4 \cdot 0.15CH_2CH_3OH$: C 61.52, H 4.66, N 10.03, found: C 61.52, H 4.48, N 9.79.

4-Bromo-*N*′-[(2,4-dihydroxyphenyl)methylidene]benzohydrazide (3e): Beige crystalline solid (0.12 g, 0.36 mmol, 71%): R_f = 0.54 (MeOH/Et_2O 1:10); mp: >250 °C (dec); ^{1}H NMR (400 MHz, [D_6]DMSO): δ = 6.32 (d, 1H, *J* = 3.0 Hz), 6.36 (dd, 1H, *J* = 8.5, 3.0 Hz), 7.32 (d, 1H, *J* = 8.5 Hz), 7.75 (d, 2H, *J* = 8.8 Hz), 7.87 (d, 2H, *J* = 8.8 Hz), 8.48 (s, 1H, C*H*N), 9.99 (s, 1H, O*H*/N*H*), 11.38 (bs, 1H, O*H*/N*H*), 11.97 ppm (bs, 1H, N*H*); ^{13}C{^{1}H} NMR (100 MHz, [D_6]DMSO): δ = 102.7, 107.8, 110.5, 128.7, 129.5, 131.3, 131.7, 136.7, 149.4 (*C*HN), 159.5 ($4C_{ar}$), 160.9 ($4C_{ar}$), 161.5 ppm (*C*=O); FTIR (KBr): $\tilde{\nu}_{max}$ = 3432 (O–H, br), 3262 (N–H, br), 3085 (C–H_{ar}, w), 1660 (C=O, sh, s), 1632 (C=N, sh, s), 1609 (C=C, sh), 1257 cm^{-1} (C–O, sh); HRMS (ESI): *m/z* $[M]^+$ calcd for $C_{14}H_{11}N_2O_3Br$: 335.0026, found: 335.0020 (difference = 0.6 mDa); Anal. calcd for $C_{14}H_{11}N_2O_3Br \cdot 0.08H_2O$: C 49.96, H 3.34, N 8.32, found: C 49.94, H 3.29, N 7.94.

4-Chloro-*N*′-[(2,4-dihydroxyphenyl)methylidene]benzohydrazide (3f): Beige crystalline solid (0.11 g, 0.37 mmol, 74%): R_f = 0.52 (MeOH/Et_2O 1:10); mp: >250 °C (dec); ^{1}H NMR (400 MHz, [D_6]DMSO): δ = 6.30 (d, 1H, *J* = 2.0 Hz), 6.33 (dd, 1H, *J* = 8.0, 2.0 Hz), 7.28 (d, 1H, *J* = 8.0 Hz), 7.59 (d, 2H, *J* = 8.5 Hz), 7.92 (d, 2H, *J* = 8.5 Hz), 8.48 (s, 1H, C*H*N), 9.99 (bs, 1H, O*H*/N*H*), 11.39 (bs, 1H, O*H*/N*H*), 11.97 ppm (bs, 1H, N*H*); ^{13}C{^{1}H} NMR (100 MHz, [D_6]DMSO): δ = 102.5, 107.6, 110.4, 128.5, 129.3, 131.2, 131.6, 136.5, 149.2 (*C*HN), 159.4 ($4C_{ar}$), 160.7 ($4C_{ar}$), 161.3 ppm (*C*=O); FTIR (KBr): $\tilde{\nu}_{max}$ = 3409 (O–H, br), 3259 (N–H, m), 3060 (C–H_{ar}, w), 1661 (C=O, sh, s), 1632 (C=N, sh, s), 1609 (C=C, sh), 1274 cm^{-1} (C–O, sh); UV/vis (DMSO): λ_{max} (ε) = 306 (15140), 340 nm (28608); HRMS (ESI): *m/z* $[M+H]^+$ calcd for $C_{14}H_{12}N_2O_3Cl$: 291.0531, found: 291.0538 (difference = −0.7 mDa); Anal. calcd for $C_{14}H_{11}N_2O_3Cl \cdot 0.17CH_2CH_3OH$: C 57.69, H 4.06, N 9.38, found: C 57.69, H 3.80, N 9.10.

(2,4-Dihydroxybenzaldehyde)dithiocarbazate (3g): Pale yellow solid (25 mg, 0.079 mmol, 16%): R_f = 0.71 (MeOH/Et_2O 1:10); mp: 190–192 °C (lit. 175–177 °C);[40] ^{1}H NMR (400 MHz, [D_6]DMSO): δ = 4.43 (s, 2H, CH_2), 6.25 (d, 1H, *J* = 1.5 Hz), 6.28 (dd, 1H, *J* = 7.0, 1.5 Hz), 7.22–7.37 (m, 6H), 8.40 (s, 1H, C*H*N), 10.00 (bs, 1H, O*H*/N*H*),

10.17 (bs, 1H, O*H*/N*H*), 13.21 ppm (bs, 1H, N*H*); $^{13}C\{^1H\}$ NMR (100 MHz, [D$_6$]DMSO): $\delta = 37.4$ (*C*H$_2$), 102.5, 108.5, 110.6, 127.3, 128.6, 129.3, 137.0, 145.9 (*C*HN), 159.2 (4C$_{ar}$), 161.7 (4C$_{ar}$), 193.8 ppm (*C*=S); FTIR (KBr): $\tilde{\nu}_{max} = 3346$ (O–H/N–H, br), 3104 (C–H$_{ar}$, m), 2972 (C–H$_{alkyl}$, m), 1627 (C=N, sh, s), 1506 (C=C, sh), 1238, 1219 (C–O, sh), 1027 cm^{-1} (C=S, sh, s); HRMS (ESI): *m/z* $[M+H]^+$ calcd for $C_{15}H_{15}N_2O_2S_2$: 319.0569, found: 319.0566 (difference = 0.4 mDa); Anal. calcd for $C_{15}H_{14}N_2O_2S_2 \cdot 0.86CH_3OH$: C 55.06, H 5.08, N 8.10, found: C 55.06, H 5.04, N 7.65.

3-[(4-Hydroxyphenyl)-methylidene]amino-1-phenylthiourea (4a): Pale yellow crystalline solid (0.20 g, 0.74 mmol, 54%): $R_f = 0.71$ (MeOH/CHCl$_3$ 1:8); mp: 195–196 °C (lit. 188–190 °C);[41] ^{1}H NMR spectroscopic data are in agreement with the reported values;[41] $^{13}C\{^1H\}$ NMR (100 MHz, [D$_6$]DMSO): $\delta = 115.6$, 125.0 (4C$_{ar}$), 125.2, 125.7, 128.0, 129.5, 139.2 (4C$_{ar}$), 143.3 (*C*HN), 159.5 (4C$_{ar}$), 175.4 ppm (*C*=S); FTIR (KBr): $\tilde{\nu}_{max} = 3293$ (O–H, m), 3210 (N–H, br), 3168 (C–H$_{ar}$, m), 2798 (C–H$_{alkyl}$, w), 1606 (C=N, sh), 1541, 1515 (C=C, sh, s), 1196 (C–O, sh, s), 1063 cm^{-1} (C=S, sh, w); HRMS (ESI): *m/z* $[M+H]^+$ calcd for $C_{14}H_{14}N_3OS$: 272.0852, found: 272.0857 (difference = −0.4 mDa); Anal. calcd for $C_{14}H_{13}N_3OS$: C 61.97, H 4.83, N 15.49, found: C 61.56, H 4.85, N 15.77.

1-(4-Chlorophenyl)-3-[(4-hydroxyphenyl)methylidene]amino-thiourea (4b): Pale yellow solid (0.19 g, 0.60 mmol, 58%): $R_f = 0.57$ (MeOH/CHCl$_3$ 1:8); mp: 199–200 °C (lit. 165–166 °C);[42] ^{1}H NMR (400 MHz, [D$_6$]DMSO): $\delta = 6.81$ (d, 2H, $J = 8.2$ Hz), 7.41 (d, 2H, $J = 8.4$ Hz), 7.63 (d, 2H, $J = 8.4$ Hz), 7.73 (d, 2H, $J = 8.2$ Hz), 8.07 (s, 1H, C*H*N), 9.95 (s, 1H, O*H*/N*H*), 10.02 (s, 1H, O*H*/N*H*), 11.74 ppm (s, 1H, N*H*); $^{13}C\{^1H\}$ NMR (100 MHz, [D$_6$]DMSO): $\delta = 115.6$, 124.9 (4C$_{ar}$), 127.2, 127.9, 129.1 (4C$_{ar}$), 129.5, 138.2 (4C$_{ar}$), 143.7 (*C*HN), 159.6 (4C$_{ar}$), 175.4 ppm (*C*=S); FTIR (KBr): $\tilde{\nu}_{max} = 3301$ (O–H, br), 3172 (N–H, br), 2986 (C–H$_{ar}$, w), 1602 (C=N, sh), 1555, 1515, 1490 (C=C, sh, s), 1269 (C–O, sh, m), 1197 (C=S, sh, m), 1093 cm^{-1} (C–Cl, sh); HRMS (ESI): *m/z* $[M+H]^+$ calcd for $C_{14}H_{13}N_3OSCl$: 306.0462, found: 306.0459 (difference = 0.3 mDa); Anal. calcd for $C_{14}H_{12}N_3OSCl \cdot 0.45H_2O$: C 53.57, H 4.14, N 13.38, found: C 53.59, H 4.27, N 13.13.

1-(4-Cyanophenyl)-3-[(4-hydroxyphenyl)methylidene]amino-thiourea (4c): Bright yellow solid (0.10 g, 0.35 mmol, 72%): $R_f = 0.67$ (MeOH/CHCl$_3$ 1:8); mp: 215–216 °C; ^{1}H NMR (400 MHz, [D$_6$]DMSO): $\delta = 6.82$ (d, 2H, $J = 8.8$ Hz), 7.73 (d, 2H, $J = 8.4$ Hz), 7.81 (d, 2H, $J = 8.8$ Hz), 7.98 (d, 2H, $J = 8.8$ Hz), 8.10 (s, 1H, C*H*N), 10.19 (bs, 1H, O*H*), 11.93 ppm (bs, 1H, N*H*); $^{13}C\{^1H\}$ NMR (100 MHz, [D$_6$]DMSO): $\delta = 106.5$ (4C$_{ar}$), 115.6, 119.0 (4C$_{ar}$), 124.7 (4C$_{ar}$), 124.7, 129.7, 132.2, 143.6 (4C$_{ar}$), 144.4 (*C*HN), 159.8 (4C$_{ar}$), 174.7 ppm (C=S); FTIR (KBr): $\tilde{\nu}_{max} = 3450$ (O–H, br), 3294 (N–H, br, m), 2231 (C≡N, sh), 1608 (C=N, sh), 1581, 1535, 1516 (C=C, sh, s), 1277 (C–O, sh), 1187 cm^{-1} (C=S, sh); HRMS (ESI): *m/z* $[M+H]^+$ calcd for $C_{15}H_{13}N_4OS$: 297.0805, found: 297.0800 (difference = 0.5 mDa); Anal. calcd for $C_{15}H_{12}N_4OS \cdot 1H_2O$: C 57.31, H 4.49, N 17.82, found: C 57.24, H 4.48, N 18.14.

1-(3-Cyanophenyl)-3-[(4-hydroxyphenyl)methylidene]amino-thiourea (4d): Yellow solid (58 mg, 0.19 mmol, 77%): $R_f = 0.60$ (MeOH/CHCl$_3$ 1:8); mp: 193–194 °C; ^{1}H NMR (400 MHz, [D$_6$]DMSO): $\delta = 6.82$ (d, 2H, $J = 8.4$ Hz), 7.56 (t, 1H, $J = 8.0$ Hz), 7.64 (d, 1H, $J = 8.0$ Hz), 7.74 (d, 2H, $J = 8.6$ Hz), 8.00 (d, 1H, $J = 8.2$ Hz), 8.09 (s, 1H), 8.11 (s, 1H, C*H*N), 9.97 (s, 1H, O*H*/N*H*), 10.15 (s, 1H, O*H*/N*H*), 11.87 ppm (s, 1H, N*H*); $^{13}C\{^1H\}$ NMR (100 MHz, [D$_6$]DMSO): $\delta = 110.7$ (4C$_{ar}$), 115.6, 118.6 (*C*≡N), 124.8 (4C$_{ar}$), 128.5, 129.3, 129.6, 130.2, 140.1 (4C$_{ar}$), 144.1 (*C*HN), 159.7 (4C$_{ar}$), 175.3 ppm (*C*=S); FTIR (KBr): $\tilde{\nu}_{max} = 3450$ (O–H, br), 3273 (N–H, m), 3100 (N–H, br), 2231 (C≡N, sh, m), 1607 (C=N, sh, m), 1543, 1515 (C=C, sh, s), 1276 (C–O, sh), 1163 cm^{-1} (C=S, sh); HRMS (ESI): *m/z* $[M+H]^+$ calcd for $C_{15}H_{13}N_4OS$: 297.0805, found: 297.0804 (difference = 0.0 mDa); Anal. calcd for $C_{15}H_{12}N_4OS \cdot 0.2H_2O$: C 60.06, H 4.17, N 18.68, found: C 60.01, H 4.22, N 18.41.

4-Hydroxy-[(4-hydroxyphenyl)methylidene]benzohydrazide (4e): Beige solid (0.20 g, 0.76 mmol, 76%): $R_f = 0.23$ (MeOH/CHCl$_3$ 1:8); mp: >250 °C (lit. 273 °C);[39] ^{1}H NMR (400 MHz, [D$_6$]DMSO): $\delta = 6.84$ (bt, 4H, $J = 8.2$ Hz), 7.54 (d, 2H, $J = 8.0$ Hz), 7.79 (d, 2H, $J = 8.8$ Hz), 8.32 (s, 1H, C*H*N), 10.00 (bs, 2H, O*H*), 11.45 ppm (s, 1H, N*H*); $^{13}C\{^1H\}$ NMR (100 MHz, [D$_6$]DMSO): $\delta = 115.7$, 115.0, 124.1 (4C$_{ar}$), 125.5 (4C$_{ar}$), 128.8, 129.6, 147.2 (*C*HN), 159.3 (4C$_{ar}$), 160.6 (4C$_{ar}$), 162.6 ppm (*C*=O); FTIR (KBr): $\tilde{\nu}_{max} = 3362$ (O–H, br, m), 3186 (N–H, br, m), 3038 (C–H$_{ar}$, m), 1609 (C=O, s), 1584 (C=N, sh), 1509 (C=C, sh, s), 1237 cm^{-1} (C–O, m); HRMS (ESI): *m/z* $[M+H]^+$ calcd for $C_{14}H_{13}N_2O_3$: 257.0921, found: 257.0918 (difference = 0.3 mDa); Anal. calcd for $C_{14}H_{12}N_2O_3 \cdot 0.4H_2O$: C 63.82, H 4.90, N 10.63, found: C 63.87, H 4.98, N 10.36.

(4-Hydroxybenzaldehyde)dithiocarbazate (4f): Bright yellow solid (0.13 g, 0.42 mmol, 43%): $R_f = 0.50$ (MeOH/CHCl$_3$ 1:8); mp: 176–177 °C; ^{1}H NMR (400 MHz, [D$_6$]DMSO): $\delta = 4.47$ (s, 2H), 6.82 (d, 2H, $J = 8.6$ Hz), 7.26 (t, 1H, $J = 7.2$ Hz), 7.33 (t, 2H, $J = 7.2$ Hz), 7.42 (d, 2H, $J = 7.2$ Hz), 7.53 (d, 2H, $J = 8.6$ Hz), 8.14 (s, 1H, C*H*N), 10.09 (bs, 1H, O*H*), 13.22 ppm (bs, 1H, N*H*); $^{13}C\{^1H\}$ NMR (100 MHz, [D$_6$]DMSO): $\delta = 37.5$ (*C*H$_2$), 115.9, 124.2 (4C$_{ar}$), 127.2, 128.5, 129.3, 129.4, 147.1 (*C*HN), 160.2 (4C$_{ar}$), 195.2 ppm (*C*=S); FTIR (KBr): $\tilde{\nu}_{max} =$ 3354 (O–H, br), 3127 (N–H, br), 3029 (C–H$_{ar}$, w), 2964 (C–H$_{alkyl}$, w), 1607 (C=N, sh, s), 1577, 1496 (C=C, sh, s), 1200 (C–O, s), 1025 cm^{-1} (C=S, sh); HRMS (ESI): *m/z* $[M+H]^+$ calcd for $C_{15}H_{15}N_2OS_2$: 303.0620, found: 303.0628 (difference = −0.8 mDa); Anal. calcd for $C_{15}H_{14}N_2OS_2$: C 59.58, H 4.67, N 9.26, found: C 59.34, H 4.66, N 9.23.

3-[(4-Methoxyphenyl)methylidene]amino-1-phenylthiourea (5a): White crystalline solid (0.20 g, 0.70 mmol, 85%): $R_f = 0.48$ (MeOH/CHCl$_3$ 1:15); mp: 179–180 °C (lit. 179 °C);[42] $^{13}C\{^1H\}$ NMR (100 MHz, [D$_6$]DMSO): $\delta = 55.3$ (*C*H$_3$O), 114.1, 125.2, 125.7, 126.6, 128.0 (4C$_{ar}$), 129.3, 139.1 (4C$_{ar}$), 142.9 (*C*HN), 160.9 (4C$_{ar}$), 175.6 ppm (4C$_{ar}$); HRMS (ESI): *m/z* $[M+H]^+$ calcd for $C_{15}H_{16}N_3OS$: 286.1009, found: 286.1008 (difference = 0.1 mDa); Anal. calcd for $C_{15}H_{15}N_3OS$: C 63.13, H 5.30, N 14.72, found: C 62.99, H 5.29, N 14.58. Spectroscopic data are in agreement with reported values.[43]

(5-Bromo-2-hydroxybenzaldehyde)dithiocarbazate (6a): Pale yellow solid (0.34 g, 0.89 mmol, 90%): $R_f = 0.52$ (MeOH/CHCl$_3$ 1:15); mp: 201–202 °C (lit. 195 °C);[44] UV/vis (DMSO): λ_{max} (ε) = 313 (11205), 329 (11776), 366 (21654), 381 nm (20076); Anal. calcd for $C_{15}H_{13}N_2OS_2Br$: C 47.25, H 3.44, N 7.35, found: C 47.19, H 3.43, N 7.24. Spectroscopic data are in agreement with reported values.[45]

General procedure for [MoO$_2$(L)MeOH] synthesis (L^1 = 3b, L^2 = 3f, L^3 = 6a): [MoO$_2$(acac)$_2$] was synthesised according to a literature procedure.[46] Equimolar amounts of the ligand and [MoO$_2$(acac)$_2$] were refluxed for 2 h in MeOH. Following partial evaporation of the solvent, the Mo^{VI} complex was isolated, washed with MeOH and dried in vacuo. Diffraction quality crystals were grown in MeOH/pentane or obtained after slow evaporation of a solution of the complex in MeOH.

MoO$_2$(L^1)MeOH (L^1 = 3b): Dark red microcrystalline solid (33 mg, 0.070 mmol, 45%): $R_f = 0.50$ (MeOH/CHCl$_3$ 1:8); mp: >250 °C (dec); ^{1}H NMR (400 MHz, [D$_6$]DMSO): $\delta = 3.17$ (d, 3H, $J = 5.3$ Hz, C*H*$_3$OH), 4.10 (q, 1H, $J = 5.1$ Hz, CH$_3$O*H*), 6.26 (d, 1H, $J = 2.2$ Hz), 6.48 (dd, 1H, $J = 8.7$, 2.2 Hz), 7.32 (d, 2H, $J = 8.0$ Hz), 7.50 (d, 1H, $J = 8.7$ Hz), 7.76 (d, 2H, $J = 8.0$ Hz), 8.66 (s, 1H, C*H*N), 9.63 (bs, 1H, O*H*/N*H*), 10.44 ppm (bs, 1H, O*H*/N*H*); $^{13}C\{^1H\}$ NMR (100 MHz, [D$_6$]DMSO): $\delta =$

48.6 (CH_3OH), 104.1, 109.8, 112.9 ($4C_{ar}$), 120.7, 125.5 ($4C_{ar}$), 128.4, 135.7, 139.8 ($4C_{ar}$), 155.2 (*C*HN), 159.1 ($4C_{ar}$), 160.7 ($4C_{ar}$), 163.7 ppm (*C*–S); FTIR (KBr): $\tilde{\nu}_{max}$ = 3394 (MeO–H, br), 3364 (N–H, br), 1596 (C=N, s), 1516 (C=C, s), 1225 (C–O, sh), 932 (O=Mo=O_{symm}, sh), 889 cm^{-1} (O=Mo=O_{asymm}, sh); UV/vis (DMSO): λ_{max} (ε) = 266 (28546), 340 (25460), 428 nm (5580); Anal. calcd for $C_{15}H_{14}N_3O_5SClMo$: C 37.55, H 2.94, N 8.76, found: C 37.47, H 2.28, N 9.17. Diffraction quality dark red needles were obtained from MeOH/pentane.

$MoO_2(L^2)$MeOH (L^2 = 3 f): Dark red crystalline solid (91 mg, 0.20 mmol, 62%): R_f = 0.54 (MeOH/$CHCl_3$ 1:8); mp: > 250 °C (dec); ^{1}H NMR (400 MHz, [D_6]DMSO): δ = 3.15 (s, 3H, CH_3OH), 4.09 (bs, 1H, CH_3OH), 6.30 (d, 1H, *J* = 2.0 Hz), 6.52 (dd, 1H, *J* = 8.6, 2.0 Hz), 7.56 (dd, 3H, *J* = 8.6, 2.0 Hz), 7.95 (d, 2H, *J* = 8.6 Hz), 8.78 (s, 1H, *CH*N), 10.64 ppm (s, 1H, *OH*); $^{13}C\{^1H\}$ NMR (100 MHz, [D_6]DMSO): δ = 48.6 (CH_3OH), 104.6, 110.4, 112.5 ($4C_{ar}$), 129.0, 129.1 ($4C_{ar}$), 129.5, 136.0, 136.4, 156.0 (*C*HN), 161.4 ($4C_{ar}$), 164.5 ($4C_{ar}$), 166.2 ppm (C–O); FTIR (KBr): $\tilde{\nu}_{max}$ = 3500 (O–H, br), 3199 (O–H, br), 1605 (C=N, sh, s), 1550 (C=C, sh, s), 1237 (C–O, sh), 932 (O=Mo=O_{symm}), 907 cm^{-1} (O=Mo=O_{asymm}); UV/vis (DMSO): λ_{max} (ε) = 326 (23590), 421 nm (7957); HRMS (ESI): *m/z* $[M-MeOH+H]^+$ calcd for $C_{14}H_{10}N_2O_5ClMo$: 418.9323, found: 418.9311 (difference = 1.2 mDa); Anal. calcd for $C_{15}H_{13}N_2O_6ClMo{\cdot}0.25H_2O$: C 39.76, H 3.00, N 6.18, found: C 39.75, H 3.51, N 5.77. Diffraction quality dark red needles were obtained from MeOH/pentane.

[$MoO_2(L^3)$MeOH] (L^3 = 6 a): Bright orange solid (0.15 g, 0.29 mmol, 89%): R_f = 0.48 (MeOH/$CHCl_3$ 1:15); mp: 218–219 °C; ^{1}H NMR (400 MHz, [D_6]DMSO): δ = 3.17 (d, 3H, *J* = 5.1 Hz, CH_3OH), 4.11 (q, 1H, *J* = 5.1 Hz, CH_3OH), 4.44 (s, 2H), 6.93 (d, 1H, *J* = 8.8 Hz), 7.27 (t, 1H, *J* = 7.3 Hz), 7.34 (t, 2H, *J* = 7.3 Hz), 7.47 (d, 2H, *J* = 7.3 Hz), 7.70 (dd, 1H, *J* = 8.8, 2.5 Hz), 8.06 (d, 1H, *J* = 2.5 Hz), 9.01 ppm (s, 1H, *CH*N); $^{13}C\{^1H\}$ NMR (100 MHz, [D_6]DMSO): δ = 37.3 (CH_2), 48.6 (CH_3OH), 112.0 ($4C_{ar}$), 120.8, 121.7 ($4C_{ar}$), 127.4, 137.0, 137.9, 136.7, 137.0, 137.9 ($4C_{ar}$), 158.7 ($4C_{ar}$), 158.8 (*C*HN), 171.0 ppm (*C*=S); FTIR (KBr): $\tilde{\nu}_{max}$ = 3337 (O–H, br), 1591 (C=N, sh, s), 1541 (C=N, sh, s), 1484, 1465 (C=C, sh, s), 1274 (C–O, sh, s), 937 (O=Mo=O_{symm}), 887 cm^{-1} (O=Mo=O_{asymm}); Anal. calcd for $C_{16}H_{15}N_2O_4S_2BrMo$: C 35.64, H 2.80, N 5.19, found: C 35.86, H 2.80, N 5.00; UV/vis (DMSO): λ_{max} (ε) = 329 (16656), 362 (13484), 380 (10051), 438 nm (1033). Diffraction quality orange needles were obtained from slow evaporation of a solution of [$MoO_2(L^3)$MeOH] in MeOH.

Synthetic procedure for [$Cu(L^4)H_2O$]: A solution of **1 i** (0.11 g, 0.32 mmol) in MeOH (5 mL) was slowly treated with an equimolar amount of $Cu(OAc)_2$ in MeOH (5 mL). The mixture was refluxed for 4 h. Following slow evaporation over a few days, [$Cu(L^4)H_2O$] was isolated as an olive-green solid (70 mg, 0.16 mmol, 53%): mp: > 250 °C (dec); FTIR (KBr): $\tilde{\nu}_{max}$ = 3362 (O–H, br), 1609 (C=N, sh, s), 1572 (C=C, sh, m), 1232 cm^{-1} (C–O, sh); UV/vis (DMSO): λ_{max} (ε) = 356 (18372), 373 (21400), 393 (24610), 413 (16886), 623 nm (135); HRMS (ESI): *m/z* $[M-H_2O+DMSO+H]^+$ calcd for $C_{16}H_{15}N_2O_5SBrCu$: 489.9254, found: 489.9246 (difference = 0.8 mDa); Anal. calcd for $C_{14}H_{11}N_2O_5BrCu$: C 39.04, H 2.57, N 6.50, found: C 39.19, H 2.37, N 6.21.

Synthesis of [$Cu(L^5)H_2O$]: A solution of **3 b** (49 mg, 0.15 mmol) in MeOH (5 mL) was treated dropwise with a solution of $Cu(OAc)_2$ (28 mg, 0.15 mmol) in MeOH (2 mL). The mixture was refluxed for 4 h. [$Cu(L^5)H_2O$] precipitated out as a brown solid (49 mg, 0.12 mmol, 80%): mp: > 250 °C (dec); FTIR (KBr): $\tilde{\nu}_{max}$ = 3373 (O–H/N–H, br), 1599 (C=N, sh, s), 1522 (C=C, sh, s), 1221 cm^{-1} (C–O, sh); UV/vis (DMSO): λ_{max} (ε) = 316 (39025), 389 (48516), 403 (42278), 590 nm (189); Anal. calcd for $C_{14}H_{12}N_3O_3SCl{\cdot}0.3H_2O$: C 41.34, H 3.12, N 10.33, found: C 41.34, H 3.13, N 10.10.

Xanthine Oxidase activity assay:[30] The assay solution contained xanthine (1 mL of 0.15 mM in H_2O) and test compounds at various concentrations made up to 3 mL with 50 mM potassium phosphate monobasic buffer (pH 7.5). The reaction was initiated by addition of the appropriate amount of xanthine oxidase (XO) to give rise to a reaction rate for the control reaction of 0.03–0.04 AU min^{-1}. The absorbance was monitored every minute for 10 min on a Jenway 6705 UV/Vis spectrophotometer with a thermostated cuvette holder set at 25 °C. The inhibitors and positive control (allopurinol) were dissolved in DMSO, with the final DMSO concentration maintained at 1% (*v/v*) of the total assay mixture. At this level, the DMSO had no appreciable effect on XO activity. The IC_{50} value was determined from analysis of dose–inhibition curves of inhibition (%) versus log [inhibitor] using Origin 6.1 software, with each assay performed in duplicate and the IC_{50} value quoted as the mean ± standard deviation (SD).

Acknowledgements

We thank the UK Biotechnology and Biological Sciences Research Council (BBSRC) and Sareum Ltd (Cambridge, UK) for financial support, Dr. Adrian Whitwood, Ms. Abeda Jamadar, Ms. Emma Dux and Mr. Robert Thatcher for crystal structure determination, and Dr. Nicola J. Smith for S-benzyldithiocarbazate synthesis.

Keywords: copper complexation · inhibitors · molybdenum complexation · schiff bases · xanthine oxidase

[1] F. Borges, E. Fernandes, F. Roleira, *Curr. Med. Chem.* **2002**, *9*, 195–217.
[2] a) P. Pacher, A. Nivorozhkin, C. Szabó, *Pharmacol. Rev.* **2006**, *58*, 87–114; b) R. Hille, *Chem. Rev.* **1996**, *96*, 2757–2816; c) M. B. Grisham, L. A. Hernandez, D. N. Granger, *Am. J. Physiol.* **1986**, *251*, G567–G574.
[3] R. Hille, T. Nishino, F. Bittner, *Coord. Chem. Rev.* **2011**, *255*, 1179–1205.
[4] C. E. Berry, J. M. Hare, *J. Physiol.* **2004**, *555*, 589–606.
[5] a) A. A. Fatokun, T. W. Stone, R. A. Smith, *Neurosci. Lett.* **2007**, *416*, 34–38; b) R. M. Wright, J. L. McManaman, J. E. Repine, *Free Radical Biol. Med.* **1999**, *26*, 348–354; c) A. T. Demiryürek, R. M. Wadsworth, *Pharmacol. Ther.* **1999**, *84*, 355–365.
[6] K. Okamoto, B. T. Eger, T. Nishino, S. Kondo, E. F. Pai, T. Nishino, *J. Biol. Chem.* **2003**, *278*, 1848–1855.
[7] a) C. Enroth, B. T. Eger, K. Okamoto, T. Nishino, E. F. Pai, *Proc. Natl. Acad. Sci. USA* **2000**, *97*, 10723–10728; b) T. Shimo, N. Ashizawa, K. Matsumoto, T. Nakazawa, O. Nagata, *Toxicol. Sci.* **2005**, *87*, 267–276; c) J. S. Cameron, H. A. Simmonds, *Br. Med. J.* **1987**, *294*, 1504–1505.
[8] a) S. Ishibuchi, H. Morimoto, T. Oe, T. Ikebe, H. Inoue, A. Fukunari, M. Kamezawa, I. Yamada, Y. Naka, *Bioorg. Med. Chem. Lett.* **2001**, *11*, 879–882; b) I. Yamada, A. Fukunari, T. Osajima, M. Kamezawa, H. Mori, J. Iwane, *Nucleosides Nucleotides Nucleic Acids* **2004**, *23*, 1123–1125.
[9] a) K. Okamoto, K. Matsumoto, R. Hille, B. T. Eger, E. F. Pai, T. Nishino, *Proc. Natl. Acad. Sci. USA* **2004**, *101*, 7931–7936; b) K. Matsumoto, K. Okamoto, N. Ashizawa, T. Nishino, *J. Pharmacol. Exp. Ther.* **2011**, *336*, 95–103.
[10] J. J. Baldwin, P. K. Lumma, F. C. Novello, G. S. Ponticello, J. M. Sprague, *J. Med. Chem.* **1977**, *20*, 1189–1193.
[11] T. Sato, N. Ashizawa, T. Iwanaga, H. Nakamura, K. Matsumoto, T. Inoue, O. Nagata, *Bioorg. Med. Chem. Lett.* **2009**, *19*, 184–187.
[12] UK National Health Service, Regional Drug and Therapeutics Centre, *New Drug Evaluation* **2010**, *101*; http://www.nyrdtc.nhs.uk/docs/nde/NDE_101_Febuxostat.pdf (Last accessed: March 14, 2011).
[13] a) Y.-T. Tung, S.-T. Chang, *J. Agric. Food Chem.* **2010**, *58*, 781–786; b) W. N. Khan, I. Ali, R. Gul, M. I. Choudhary, *Chem. Nat. Compd.* **2008**, *44*, 95–97; c) J. M. Pauff, R. Hille, *J. Nat. Prod.* **2009**, *72*, 725–731; d) L. D. Kong, Y. Zhang, X. Pan, R. X. Tan, C. H. K. Cheng, *Cell. Mol. Life Sci.* **2000**, *57*, 500–505.
[14] C.-Y. Hsieh, S.-T. Chang, *J. Agric. Food Chem.* **2010**, *58*, 1578–1583.

[15] a) P. L. Owen, T. Johns, *J. Ethnopharmacol.* **1999**, *64*, 149 – 160; b) J. Havlik, R. G. d. I Huebra, K. Hejtmankova, J. Fernandez, J. Simonova, M. Melich, V. Rada, *J. Ethnopharmacol.* **2010**, *132*, 461 – 465.
[16] a) C.-M. Lin, C.-S. Chen, C.-T. Chen, Y.-C. Liang, J.-K. Lin, *Biochem. Biophys. Res. Commun.* **2002**, *294*, 167 – 172; b) Y.-C. Chang, F.-W . Lee, C.-S. Chen, S.-T. Huang, S.-H. Tsai, S.-H. Huang, C.-M. Lin, *Free Radical Biol. Med.* **2007**, *43*, 1541 – 1551.
[17] M. Leigh, C. E. Castillo, D. J. Raines, A. K. Duhme-Klair, *ChemMedChem* **2011**, *6*, 612 – 616.
[18] a) Z.-L. You, D.-H. Shi, H.-L. Zhu, *Inorg. Chem. Commun.* **2006**, *9*, 642 – 644; b) Y.-G. Li, H.-L. Zhu, H. Yan, S. W. Ng, *Inorg. Chim. Acta* **2007**, *360*, 2881 – 2889; c) Z.-L. You, D.-H. Shi, . C. Xu, Q. Zhang, H.-L. Zhu, *Eur. J. Med. Chem.* **2008**, *43*, 862 – 871; d) Y.-Q. Cui, Z.-L. You, X.-F. Li, X.-L. Wang, Y.-P. Ma, . C. Wang, C.-L. Zhang, *Trans. Met. Chem.* **2010**, *35*, 159 – 163.
[19] Y. Niu, H. Zhu, J. Liu, H. Fan, L. Sun, W. Lu, X. Liu, L. Li, *Chem. Biol. Interact.* **2011**, *189*, 161 – 166.
[20] a) S. Chaves, G. Marco, S. Canario, R. Jellic, M. Joao Romao, J. Trincao, E. Herdtweck, J. Sousa, C. Diniz, P. Fresco, A. Santos, *Dalton Trans.* **2008**, 1773 – 1782; b) A. Fukunari, K. Okamoto, T. Nishino, B. T. Eger, E. F. Pai, M. Kamezawa, I. Yamada, N. Kato, *J. Pharmacol. Exp. Ther.* **2004**, *311*, 519 – 528.
[21] a) I. Sheikhshoaie, A. Rezaeifard, N. Monadi, S. Kaafi, *Polyhedron* **2009**, *28*, 733 – 738; b) L. Sinclair, J. U. Monda, D. Uhrhammer, F. A. Schultz, *Inorg. Chim. Acta* **1998**, *278*, 1 – 5; c) K. Nakajima, K. Yokoyama, T. Kano, M. Kojima, *Inorg. Chim. Acta* **1998**, *282*, 209 – 216; d) A. Syamal, M. R. Maurya, *Coord. Chem. Rev.* **1989**, *95*, 183 – 238; e) J. Liimatainen, A. Lehtonen, R. Sillanpää, *Polyhedron* **2000**, *19*, 1133 – 1138.
[22] A. Rezaeifard, I. Sheikhshoaie, N. Monadi, M. Alipour, *Polyhedron* **2010**, *29*, 2703 – 2709.
[23] K. Okamoto, B. T. Eger, T. Nishino, E. F. Pai, T. Nishino, *Nucleosides Nucleotides Nucleic Acids* **2008**, *27*, 888 – 893.
[24] a) M. R. Maurya, N. N. Jayaswal, V. G. Puranik, P, Chakrabarti, S. Gopinathan, C. Gopinathan, *Polyhedron* **1997**, *16*, 3977 – 3983; b) S. Gupta, A. K. Barik, S. Pal, A. Hazra, S. Roy, R. J. Butcher, S. K. Kar, *Polyhedron* **2007**, *26*, 133 – 141.
[25] A. A. Soliman, S. A. Ali, A. Orabi, *Spectrochim. Acta, Part A* **2006**, *65*, 841 – 845.
[26] Y. Sui, X. Zeng, X. Fang, X. Fu, Y. Xiao, L. Chen, M. Li, S. Cheng, *J. Mol. Catal. A: Chem.* **2007**, *270*, 61 – 67.
[27] a) M. Kato, K. Nakajima, Y. Yoshikawa, M. Hirotsu, M. Kojima, *Inorg. Chim. Acta* **2000**, *311*, 69 – 74; b) W. E. Hill, N. A. Atabay, C. S. McAuliffe, F. P. McCullough, S. M. Razzoki, *Inorg. Chim. Acta* **1979**, *35*, 35 – 41.
[28] M. Cindrić, G. Galin, D. Matković-Čalogović, P. Novak, T. Hrenar, I. Ljubić, T. K. Novak, *Polyhedron* **2009**, *28*, 562 – 568.
[29] N. R. Pramanik, S. Ghosh, T. K. Raychaydhuri, S. Ray, R. J. Butcher, S. Mandal, *Polyhedron* **2004**, *23*, 1595 – 1603.
[30] *Methods of Enzymatic Analysis, 2nd ed.*, (Ed.: H. U. Bergmeyer, K. Gawehn, M. Grassi), Academic Press, New York, **1974**.
[31] A. P. Sweeney, S. G. Wyllie, R. A. Shalliker, J. L. Markham, *J. Ethnopharmacol.* **2001**, *75*, 273 – 277.
[32] a) F. J. Philpot, *Biochem. J.* **1938**, *32*, 2013 – 2016; b) M. S. Mondal, S. Mitra, *J. Inorg. Biochem.* **1996**, *62*, 271 – 279; c) A. M. Ghe, C. Stefanelli, D. Carati, *Talanta* **1984**, *31*, 241 – 247.
[33] a) R. Mukhopadhyay, S. Bhattacharjee, R. J. Bhattacharyya, *Chem. Soc. Dalton Trans.* **1994**, 2799 – 2804; b) H. Beraldo, L. P. Boyd, D. X. West, *Trans. Met. Chem.* **1997**, *23*, 67 – 71; c) R. M. El-Bahnasawy, E.-S. El-Shereafy, T. I. Kashar, *Trans. Met. Chem.* **1995**, *20*, 104 – 106.
[34] a) U. Kela, R. Vijayvargiya, *Biochem. J.* **1981**, *193*, 799 – 803; b) M. S. Mondal, A. K. Sau, S. Mitra, *Biochim. Biophys. Acta* **2000**, *1480*, 302 – 310; c) A. A. J. Saboury, *J. Iran. Chem. Soc.* **2009**, *6*, 219 – 229.
[35] A. K. Sau, M. S. Mondal, S. Mitra, *Biochim. Biophys. Acta* **2001**, *1544*, 89 – 95.
[36] a) A. W. Girott, J. P. Thoma, J. E. Hordan, *J. Free Radicals Biol. Med.* **1985**, *1*, 395 – 401; b) M. Ciuffi, C. Cellai, S. Franci-Micheli, P. Failli, L. Zillett, M. Ginanneschi, M. Chelli, A. M. Papini, F. Paoletti, *Pharmacol. Res.* **1998**, *38*, 279 – 287.
[37] M. Akbar Ali, M. T. H. J. Tarafdar, *Inorg. Nucl. Chem.* **1977**, *39*, 1785 – 1791.
[38] E. Franzen, *J. Prakt. Chem.* **1910**, *2*, 248.
[39] N. P. Buu-Hoï; N. D. Xuong, N. H. Nam, F. Binon, R. J. Royer, *J. Chem. Soc.* **1953**, 1358 – 1364.
[40] O. S. Abu-Team, N. M. Rateb, A. O. Abdelhamid, *Phophorus Sulfur Silicon Relat. Elem.* **2003**, *178*, 2363 – 2371.
[41] K. Krishnan, K. Prathiba, V. Jayaprakash, A. Basu, N. Mishra, N. Zhou, S. Hu, Y. Yen, *Bioorg. Med. Chem. Lett.* **2008**, *18*, 6248 – 6250.
[42] I. D. Shah, J. P. Trivedi, *J. Indian Chem. Soc.* **1963**, *40*, 889 – 893.
[43] K. M. M. S. Prakash, L. D. Prabhakar, D. V. Reddy, *Analyst* **1986**, *111*, 1301 – 1306.
[44] S. K. Pandit, S. Gopinathan, C. Gopinathan, *Indian J. Chem., Sect. A: Inorg., Phys., Theor. Anal.* **1982**, *21*, 1004 – 1006.
[45] M. R. Maurya, S. Khurana, A. Shailendra, W. Zhang, D. Rehder, *Eur. J. Inorg. Chem.* **2003**, 1966 – 1973.
[46] G. J. Chen, J. W. McDonald, W. E. Newton, *Inorg. Chem.* **1976**, *15*, 2612 – 2615.

Received: February 3, 2011
Published online on April 8, 2011

